

# 主論文

Geochemical characteristics of Archean cherts and  
other sedimentary rocks in the Pilbara Block, Western  
Australia: Evidence for the Archean sea-water enriched in  
hydrothermally-derived iron and silica

*Precambrian Research*(in press)

(始生代のチャートの化学組成から示される太古海洋の熱水活動)

杉谷 健一郎

名古屋大学図書	
洋	1068486

Geochemical characteristics of Archean cherts and  
other sedimentary rocks in the Pilbara Block,  
Western Australia: evidence for the Archean sea-  
water enriched in hydrothermally-derived  
iron and silica

Kenichiro Sugitani\*

*Department of Earth Sciences, Nagoya University,*

*Nagoya 464-01, Japan*

\*present address

*Department of Geology, College of General Education,*

*Nagoya University, Nagoya 464-01, Japan*

## Abstract

Geochemical and mineralogical characteristics of Archean sedimentary rocks such as cherts, banded iron-formations (BIFs), shales and sandstones collected from the Pilbara Block, Western Australia were studied. Lithologic features of various types of chert occurring within the Pilbara Supergroup are closely related to their chemical compositions. Red and brown bands of banded cherts generally show higher  $\text{Fe}_2\text{O}_3^*$  (total iron as  $\text{Fe}_2\text{O}_3$ ) than do other cherts, whereas grey, greenish-grey and pale yellowish-grey cherts are characteristic of relatively higher concentrations of Al and Ti. White cherts are generally composed almost exclusively of  $\text{SiO}_2$ .

Geochemical characteristics of the cherts suggest that they were precipitated from hydrothermal solutions. Evidence for the hydrothermal origin includes (1) low  $\text{MnO}/\text{Fe}_2\text{O}_3^*$  values, (2) low contents of heavy metals, (3) positive Eu-anomalies, (4) low Co/Zn and Ni/Zn values and (5) high concentrations of Mn and Fe in carbonates. Positive correlations between Fe and heavy metals such as Ni and Zn imply the intermittent precipitation of Fe-oxides (hydroxides) along with these heavy metals in the ancient ocean. Cherts, except for grey, greenish-grey and pale yellowish-grey cherts, are highly depleted in detrital materials. This may have been caused by rapid precipitation of hydrothermally-derived Fe and Si. The Archean "Pilbara Ocean" is believed to have been enriched in Fe and Si derived from hydrothermal activity.

## Introduction

Few studies of the chemical aspects of Archean cherts have been made, although Archean sedimentary rocks, particularly banded iron-formations and shales have often been studied in relation to oceanic, atmospheric and crustal evolution of the early history of the Earth. This is probably because of the very low concentration of constituent elements other than Si in chert. Systematic sampling of Archean cherts from various geological settings and the detailed chemical analyses and microscopic examinations, however, are crucial for their origins and depositional environments.

This paper is intended to describe chemical and mineralogical characteristics of Archean cherts together with some associated sedimentary rocks collected from the Warrawoona and Gorge Creek Groups in the Pilbara Block, Western Australia. Samples collected from the Warrawoona Group in the early Archean are used mainly for the discussion, and those from the Gorge Creek Group for reference.

The following points are discussed on the basis of chemical and mineralogical data in this paper: (1) origins and depositional environments of Archean cherts in the Pilbara Block; (2) origins of detrital materials in them and crustal developments in the Pilbara Block; (3) regional differences in the chemistry of sedimentary rocks within the Pilbara Block.

## Geological setting and field observation

The Pilbara Block is one of the oldest cratons on the Earth and consists of a granite-gneiss complex and surrounding greenstone belt (Fig. 1). This greenstone belt is composed of the Pilbara Supergroup which is subdivided into three major rock units, the

Warrawoona, Gorge Creek and Whim Creek Groups in ascending order (Hickman, 1983). The Warrawoona Group consists of ultramafic, tholeiitic, felsic lavas and volcanoclastic rocks with subordinate chert. Zircon U-Pb systems in dacite of the Duffer Formation, the middle member of the group, indicate an age of 3.45 Ga. (Pidgeon, 1978). The Gorge Creek Group consists dominantly of sedimentary rocks such as shale, sandstone, conglomerate and BIF. After the deposition, the Gorge Creek Group was deformed and the major domal structures of the Pilbara Block were developed. The deformation and metamorphism are considered to have continued till 2.95 Ga (Oversby, 1976). The Whim Creek Group, composed essentially of volcanic rocks, lies unconformably over the two Groups in the western part of the Pilbara Block. Samples for this study were collected from three locations in the Warrawoona Group and from two locations in the Gorge Creek Group, (Fig. 1 and Table 1). The geological outline of the sampling locations is given below.

### *The Warrawoona Group*

Red-white-grey banded chert layers occur at Marble Bar (Loc. 1, Fig. 1). This chert unit is a member of the Towers Formation that overlies felsic volcanic rocks and volcanoclastic rocks of the Duffer and Panorama Formations (DiMarco and Lowe, 1989). These three Formations are intercalated in greenstone units. Samples were collected from a chert outcrop about 20m thick.

Thin chert layers intercalated in ultramafic-mafic volcanic rocks occur within various parts of the Warrawoona Group. Banded red-white-grey and greenish-grey chert layers occur within pillow basalt 45km northwest of Marble Bar (Loc. 2, Fig. 1) at the location denoted as "Pillow Hill" (in this study). These chert layers are associated with

the Euro Basalt of the Warrawoona Group (Hickman et al., 1983). The thickness of this banded chert unit is approximately 5m.

Variiegated chert layers occur 3km west of Roebourne (Loc. 3, Fig. 1). Samples were taken from this chert unit, which is about 20m thick, and which overlies amphibolite-facies mafic volcanic rocks of the Talga Talga Subgroup. This chert unit is stratigraphically correlative to the Marble Bar Chert.

### *The Gorge Creek Group*

Cherts, BIFs, shales, sandstones and conglomerates occur at Coppin Gap, 50km northeast of Marble Bar (Loc. 4, Fig. 1). They overlie silicified pillow basalts and komatiites. The thickness of this sedimentary sequence is estimated to be 50m.

Cherts, BIFs and shales are exposed at Point Samson, 20 km north-northeast of Roebourne (Loc. 5, Fig. 1). Conglomerate does not occur. BIF and a shale-dominant unit overlies a chert-dominant unit at this outcrop which is about 100m wide. Sedimentary rocks at these two outcrops are members of the Cleaverville Formation of the Gorge Creek Group.

## Sample Description

All samples were examined with the optical microscope, and some were analysed by X-ray diffractometry using Cu-K $\alpha$  radiation. Lithologies of samples at each outcrop are listed in Table 1.

Sedimentary rocks in most Archean terranes such as the Yilgarn Block, Western Australia, and the Isua Supracrustal Belt, West Greenland, have generally undergone a wide range of metamorphism up to the amphibolite facies grade (Dymek and Klein,

1988; Gole, 1981). In contrast, most sedimentary rocks from the Pilbara Block studied here show little evidence of high-grade metamorphism. Their original chemical and mineralogical features are expected not to have been strongly altered. Some minerals, however, are altered or silicified, and the primary minerals were identified on the basis of shapes and textures and by comparisons with illustrations in previous studies. Lithologic features examined in the field also imply that some rocks, grey and pale yellowish-grey in color, may well be silicified clastic sediments. These, however, are composed mostly of Si as described later and therefore are denoted as "chert" for convenience in this study.

### *Marble Bar*

Red-white-grey banded cherts are dominant varieties at Marble Bar, and the thickness of most bands ranges from 1 to 10 cm. Red-white banded chert layers are sporadically intruded by grey (dark grey-light grey) cherts, where angular blocks of red-white banded chert are included in massive grey cherts. Forty five chert samples and one greenstone sample were collected and analysed.

The color variations of the red-white banded cherts are attributed essentially to their mineral composition. The red (actually red, reddish-brown, brownish-yellow) bands contain generally hematite, goethite, opaque minerals, rhombic carbonate (hematite or goethite pseudomorph after dolomite) and possible altered pyrite and magnetite, whereas the white bands consist mostly of fine-grained quartz. Fine laminae are seen in red bands. Hematite occurs as fine grains or patches in red bands, and the fine hematite grains sporadically aggregate and form peloidal structure (Fig. 2a). Some red bands contain fine particles with high refractive index, and these particles, although unidentified, may be carbonates. A grain of hematite pseudomorph was detected under the microscope at

the boundary between red and white bands (Fig. 2b). Similar-shaped pseudomorphs were identified as gypsum or anhydrite by Buick and Dunlop (1990) and Lowe (1983).

Grey cherts associated with red-white banded cherts generally contain more sericite, chlorite and rutile than the red-white banded cherts, and are enriched in carbonaceous matter (Fig. 2c). They contain sparsely distributed euhedral pyrite grains. Some of them contain lenticular ghosts (Fig. 2d) that are possibly silicified gypsum grains (Lowe and Knauth, 1977; Lougheed, 1983). A thin clastic layer 5mm thick was found in light grey chert (Fig. 2e); this layer contains sericite, detrital quartz, zircon and rutile (Fig. 2f).

### *Pillow Hill*

Well-stratified, red-white-grey chert layers occur within pillow basalt. They can be subdivided into three distinct types on the basis of lithologic features; greenish-grey chert, red-white-grey banded chert and tuffaceous chert.

Greenish-grey cherts lie directly on greenstones, and are overlain by red-white-grey banded cherts. Tuffaceous cherts, greenish-brown in color, are sporadically intercalated with red-white-grey banded cherts. Each band of the red-white-grey banded cherts is thinner than 10cm. These chert bands generally contain rhombic crystals of dolomite or ankerite (Fig. 3a). Banded cherts (12 samples), greenish-grey cherts (3 samples) and greenstones (2 samples) were selected for this study.

Basal greenish-grey cherts (Fig. 3b) consist of very fine-grained quartz, opaque minerals, rhombic carbonate crystals, sericite and chlorite. Elongated cavities, possibly silicified carbonates, are usually detected under the microscope. Some of the rhombic carbonate crystals have been silicified and replaced by quartz. Fine opaque minerals

are possibly pyrite. Red bands of the banded chert contain very fine-grained hematite forming peloidal structure (Fig. 3c) like that in the red-bands of the Marble Bar Chert (Fig. 2a). White bands of the banded chert consist mostly of fine-grained quartz. Euhedral pyrite grains are scattered throughout both in the red-white-grey banded and greenish-grey cherts.

### *Roebourne*

Lithologic features of the chert layers occurring at Roebourne are distinctly different from those of the Marble Bar Chert. Various types of chert occur at this outcrop. They are structurally banded, laminated and massive, and white, pale yellowish-grey, grey, black and brown in color. Dominant lithologies are banded white, pale yellowish-grey and grey cherts. A thin conglomerate-like layer, which contains detrital quartz grains in a ferruginous matrix, occurs also. Twelve chert samples were collected and analysed.

Banded chert consists of rhythmic alternation of yellowish-brown, brown and white bands thinner than 10cm. Hematite, magnetite and goethite occur in the yellowish-brown and brown bands (Fig. 3d). The black and white laminated cherts consist of alternating of black dusty bands containing unidentified fine particles and white, quartz-dominated bands. Pale yellowish-grey cherts contain abundant sericite, whereas white cherts consist mostly of fine-grained quartz, and sericite is rare. Grey chert contains sericite and chlorite.

### *Coppin Gap and Point Samson*

At Coppin Gap, cherts occur dominantly with subordinate amounts of BIFs, silty shales, sandstones and conglomerates. Some of the rocks have been metamorphosed

and recrystallized. Most of the cherts are laminated and are composed of alternations of grey and black bands. Silty shales consist largely of detrital quartz grains and chert fragments in a matrix of sericite, hematite and fine-grained quartz. Detrital zircon and rutile can be seen in silty shale and sandstone. Angular chert blocks and rounded orthoquartzite fragments, of various sizes, are set in a ferruginous matrix of conglomerate. BIFs (3 samples), silty shales (3 samples) and sandstone (1 sample) were selected for analyses.

Cherts and BIFs with minor amounts of shales are exposed at Point Samson, where conglomerate and sandstone do not occur. Samples from this outcrop are fairly weathered, and most shales are deeply weathered and friable. BIFs (14 samples) and shales (3 samples) were selected for this study. BIFs consist of alternating red-brown and white bands thinner than 1cm. The red-brown bands contain hematite, goethite and siderite, whereas the white bands contain very little. BIFs from this outcrop contain more clay minerals such as sericite than do other red-white banded cherts.

## Analytical procedures and results

Fragments of rock samples about 1cm in size were crushed with a jaw crusher and sieved using 80 mesh. Fragments larger than 80 mesh were ground finer than 120 mesh with an agate mortar.

Major and minor components were analysed using an automatic X-ray fluorescence spectrometer by the method of Sugisaki et al. (1977, 1981). Rare earth elements (REE) were analysed using an ICP mass spectrometer. Ferrous iron, CO<sub>2</sub> and H<sub>2</sub>O were also determined by the method of Sugisaki (1981). The chemical composition of the minerals

was determined with an electron microprobe. Analytical results are listed in Tables 2, 3, 4 and 5.

## Geochemical description of the present samples

Samples from the Pilbara Block, except for shales and sandstone, consist mostly of Si and Fe, and the concentrations of other elements are generally low. Most samples show extremely low concentrations of Ti which is usually contained in detrital materials; Ti-levels of most samples are much lower than those for Phanerozoic biogenic and hydrothermal cherts (Fig. 4). Grey, greenish-grey and pale yellowish-grey cherts and samples from Point Samson, however, are exceptional. These grey, greenish-grey and pale yellowish-grey cherts tend to be enriched in  $\text{Al}_2\text{O}_3$  and Zr as well as  $\text{TiO}_2$  compared with associated cherts (Fig. 5).

Concentrations of  $\text{Fe}_2\text{O}_3^*$  in some samples are higher than 10% (Table 2). These Fe-rich samples, in contrast with Fe-poor ones, tend to be enriched in Co, Ni, Cu, Zn, Y, Al and P. Even though enrichment of Mn is also found in some Fe-rich samples, most of them are characterised with low  $\text{MnO}/\text{Fe}_2\text{O}_3^*$  values ( $<0.05$ ) (Table 2). It should be noted that Ni and Zn are positively correlated with  $\text{Fe}_2\text{O}_3^*$  in the samples, except for the Pillow Hill samples, and grey, pale-yellowish grey cherts and clastic sediments from the other locations (Fig. 6). Most of the present Fe-rich samples, moreover, show a Zn-enrichment relative to Ni and Co (Table 6). REE were determined for two samples from Marble Bar (1B-18) and Pillow Hill (2B-10), both of which contain fine-grained hematite and show peloidal structure (Figs. 2a and 3c). Chondrite-normalized REE patterns in them show slight positive Eu-anomalies (Fig. 7).

Histograms of  $\text{Al}_2\text{O}_3/\text{TiO}_2$  values for the samples studied are shown in Fig. 8. These oxides neither dissolve nor precipitate through normal weathering and depositional processes and silicification (Duchač and Hanor, 1987); their mutual ratio, consequently, tends to be constant. The  $\text{Al}_2\text{O}_3/\text{TiO}_2$  value, therefore, is an indicator of the source of their detrital components in sedimentary rocks and marine sediments (Ewers and Morris, 1981; Sugisaki et al., 1982). This ratio will be discussed subsequently.

### *Marble Bar*

Color variations of the cherts from Marble Bar are attributed to their Fe-contents and mineral assemblages in each band. Red bands (1-B15 ~ 1-B31) of the red-white banded cherts generally contain more  $\text{Fe}_2\text{O}_3^*$  (total iron as  $\text{Fe}_2\text{O}_3^*$ ) than do adjoining white ones (1-B1 ~ 1-B14). Red bands in the red-white banded cherts with more than 10%  $\text{Fe}_2\text{O}_3^*$  are chemically designated as red cherts, and the others as white cherts. Grey cherts (1-G1 ~ 1-G14), on the other hand, are depleted in Fe ( $\text{Fe}_2\text{O}_3^* < 10\%$ ), and generally contain more  $\text{Al}_2\text{O}_3$ ,  $\text{TiO}_2$  and Zr in comparison with white cherts (Fig. 5). Some grey cherts contain Ni, Co, and Zn more than do white cherts in spite of their low  $\text{Fe}_2\text{O}_3^*$  contents. The difference in interelement relationships between red-white banded cherts and grey cherts, is noteworthy; Ni and Zn are positively correlated with  $\text{Fe}_2\text{O}_3^*$  in red-white banded cherts as described above, but with  $\text{TiO}_2$  in grey cherts (Fig. 9).

The  $\text{Al}_2\text{O}_3/\text{TiO}_2$  values in the Marble Bar Chert cluster mainly around 20 (Fig. 8a), which is higher than the value for a greenstone (7 for 1-Gs) collected from Marble Bar. It should be noted that the ratios in Fe-rich red cherts ( $\text{Fe}_2\text{O}_3^* > 10\%$ ) do not converge on a fixed value. The high  $\text{Al}_2\text{O}_3/\text{TiO}_2$  values in the red cherts could be ascribed to Al-uptake on the surface of Fe-oxides or hydroxides (Lövgren et al., 1990). Microprobe

analyses indicated that significant amounts of Al in red cherts are incorporated into Fe-oxides such as hematite (Table 5). The  $\text{Al}_2\text{O}_3/\text{TiO}_2$  values in Fe-rich samples, therefore, can not always be considered to be representative of the values in detrital components.

### *Pillow Hill*

Red-white-grey banded cherts from Pillow Hill resemble the cherts from Marble Bar in appearance and are depleted in  $\text{Al}_2\text{O}_3$  and  $\text{TiO}_2$  (<0.1% and <0.01%, respectively). The concentrations of  $\text{Fe}_2\text{O}_3^*$  in the cherts, however, do not exceed 10%, and no remarkable differences in chemical compositions between red-white cherts and grey ones are recognised for these samples. Red-white-grey chert sequences (2-B1 ~ 2-B12) from Pillow Hill are conspicuously enriched in Mg and Ca (average 0.75 and 1.96, respectively) compared with the other cherts (Table 2). Rhombic carbonate minerals such as ankerite and dolomite (Fig. 3a) are responsible for the enrichments of Mg and Ca in the cherts. These carbonates show high concentrations of Fe and Mn (Table 4). Red-white-grey banded cherts are remarkably enriched in Pb and Zn relative to  $\text{TiO}_2$  when compared with other cherts with less than 10%  $\text{Fe}_2\text{O}_3^*$  studied here and Phanerozoic biogenic Kamiaso and hydrothermal Franciscan cherts (Fig. 10). Greenish-grey cherts (2-Gr1 ~ 2-Gr3) contain more  $\text{Al}_2\text{O}_3$ ,  $\text{TiO}_2$  and possibly Zr than do red-white-grey banded cherts (Fig. 5b).

The  $\text{Al}_2\text{O}_3/\text{TiO}_2$  values in Pillow Hill tend to be lower than those in Marble Bar (Fig. 8a). These values range between the values for the associated greenstones (25 for 2-Gs1 and 9 for 2-Gs2).

### *Roebourne*

Nickel and Zn in the samples, except for grey and pale yellowish-grey cherts, are positively correlated with  $\text{Fe}_2\text{O}_3^*$ , whereas Cr is not (Fig. 6b). Three cherts (3-G, 3-PY1, 3-PY2), grey and pale yellowish-grey in color, contain more Al, Ti, K and Cr than do other samples (Fig. 5c and Table 2). It is remarked that concentrations of Al, Ti, Fe, Mg and Zr are higher in the black band (3-L2) than in white one (3-L1) of the laminated chert. The  $\text{Al}_2\text{O}_3/\text{TiO}_2$  values fluctuate widely in the Roebourne samples (Fig. 8a). Pale yellowish-grey cherts have high  $\text{Al}_2\text{O}_3/\text{TiO}_2$  values ( $>70$ ), and grey chert has a smaller value (22) (Table 2).

#### *Coppin Gap and Point Samson*

Nickel and Zn are positively correlated with  $\text{Fe}_2\text{O}_3^*$  in the most samples except for the shales and sandstone from Point Samson (Fig. 6c). Weakly positive correlations between Cr and  $\text{Fe}_2\text{O}_3^*$  can be seen, whereas such correlation is not found in samples from Marble Bar and Roebourne (Figs. 6a and b). The interelement-relationships are not evident for Coppin Gap BIFs.

Red-brown bands of BIFs (5-I1 ~ 5-I11) from Point Samson contain more Al, Ti, Mg, K and Zr than do Fe-rich samples from other locations. Positive correlations between  $\text{TiO}_2$  and other elements such as  $\text{K}_2\text{O}$  and  $\text{MgO}$  are present, but the elements/ $\text{TiO}_2$  values in BIF samples are generally different from those for shales (Fig. 11). The  $\text{Al}_2\text{O}_3/\text{TiO}_2$  values in the BIF samples from Coppin Gap (4-I1, 4-I3) range between 18 and 22, and are close to the range of shales and sandstone (16-24) (Fig. 8a). High variability in  $\text{Al}_2\text{O}_3/\text{TiO}_2$  values (Fig. 8a) is a persistent feature of samples occurring from Point Samson.

Samples of shale and sandstone were collected exclusively from these two outcrops.

Such clastic rocks were not found at the other locations. The clastic rocks show a correlation between  $\text{Al}_2\text{O}_3/\text{TiO}_2$  and  $\text{K}_2\text{O}/\text{TiO}_2$ . Other data collected from the Pilbara Block (McLennan et al., 1983) show the same trend noted in the present samples (Fig. 12).

## Origins of the present cherts and BIFs

Most of the present Archean ferruginous sedimentary rocks (Fe-rich samples; Fe-rich chert and BIF containing more than 10%  $\text{Fe}_2\text{O}_3^*$ ) have probably been deposited orthochemically from a solution with little contribution of detrital materials as indicated by extremely low concentrations of  $\text{TiO}_2$  (Fig. 4). The chemical data show that these rocks in the Pilbara Block had been formed under hydrothermal influences.

Chemical evidence for a possible hydrothermal origin of the present samples includes; (1) low  $\text{MnO}/\text{Fe}_2\text{O}_3^*$  values, (2) low concentrations of heavy metals, (3) positive Eu-anomalies, and (4) low  $\text{Ni}/\text{Zn}$  and  $\text{Co}/\text{Zn}$  values.

Low  $\text{MnO}/\text{Fe}_2\text{O}_3^*$  values (Table 2) and low concentrations of heavy metals are widely accepted as the general characteristics of Phanerozoic hydrothermal deposits. The positive Eu-anomalies shown by red cherts from Marble Bar and Pillow Hill (Fig. 7) can be attributed to hydrothermal components. The Eu-anomalies in Early Proterozoic and Archean BIFs are ascribed to a hydrothermal input into the solution from which they were precipitated (Fryer, 1983; Dymek and Klein, 1988; Beukes and Klein, 1990). The  $\text{Ni}/\text{Zn}$  and  $\text{Co}/\text{Zn}$  values of hydrothermal deposits are lower than those of Phanerozoic deep-sea ferromanganese nodules (Toth, 1980; Sugitani et al., 1991), and both values in the present ferruginous sedimentary rocks are also lower than those in the nodules (Table 6). Toth (1980) suggested that hydrothermal solutions might be enriched in Zn relative

to other metals. Most silica in the present chert layers may have been derived from hydrothermal solutions enriched in Si as well as Fe. Amorphous silica and quartz in hydrothermal deposits have been reported by some workers (Haymon and Kastner, 1981; Canadian American Seamount Expedition, 1985). In the Galapagos hydrothermal field, Herzig et al. (1988) found chimneys composed of pure amorphous silica, products of direct precipitation from hydrothermal solutions. Hydrothermal cherts occur in Phanerozoic strata on land (Yamamoto, 1987; Sugitani et al., 1991) and within marine sediments (Adachi et al., 1986).

Nickel and Zn have a positive correlation with  $\text{Fe}_2\text{O}_3^*$  in the samples studied except for grey and greenish-grey cherts and clastic sediments (Fig. 6). Adsorption of heavy metals on the surface of Fe-oxides (hydroxides) (e.g. Balistrieri and Murray, 1982) may account for these positive correlation. Mn-uptake on the goethite (Stiers and Schwertmann, 1985) and coprecipitation of P with Fe-hydroxides as in the hydrothermal systems (Marchig et al., 1982), may also be responsible for Mn and P enrichments of some red cherts. A positive correlation between Fe and Ni is found also in some of Phanerozoic hydrothermal deposits (Robertson and Hudson, 1973; Varnavas and Panagos, 1984). These facts and the iron-silica banding indicate that intermittent precipitation of Fe-oxides along with some elements took place in an ancient ocean.

Fe-rich samples with more than 30%  $\text{Fe}_2\text{O}_3^*$  are typical BIFs. Relative abundances of some elements in the samples from Marble Bar and Point Samson are somewhat different from those compiled by Gole and Klein (1981), who suggested a common and unique depositional mechanism for BIFs based on the uniform composition of BIFs from various geological settings. The present ferruginous sedimentary rocks are depleted

in Mg and Ca compared with data by Gole and Klein (1981) and Dymek and Klein (1988)(Fig. 13). The depletion in Mg and Ca in the present Pilbara samples, however, is not regarded as a common feature for Archean BIFs but a regional one, because Archean BIFs from the Isua Supracrustal Belt, West Greenland (Dymek and Klein, 1988) and the Yilgarn Block, Western Australia (Gole, 1981) are chemically similar to those compiled by Gole and Klein (1981). Archean BIFs from the Isua and the Yilgarn do not show the interelement relationships (Fe-Ni, Fe-Zn) found in the present samples. Numerous data from BIFs of various types produced by Gross and McLeod (1980) also suggest that Fe does not correlate with Ni and Zn in many cases. The positive correlation of Fe with Ni and Zn, therefore, characterises only of the Pilbara ferruginous sedimentary rocks.

## Characteristics of sampled areas

### *Marble Bar*

Red-white banding in the Marble Bar Chert is ascribed to intermittent precipitation of amorphous Fe-oxides along with some heavy metals, Y, Al, Mn and P, as discussed above. In contrast, grey cherts containing clay minerals, and carbonaceous matters are remarkably different in origin. The chemical differentiation between the two types of cherts may, at least partially, be due to the larger contribution of detrital components to grey cherts relative to red-white banded cherts shown by the high concentrations of  $\text{TiO}_2$ ,  $\text{Al}_2\text{O}_3$  and Zr in them (Fig. 5). The detrital materials in the cherts must have been derived not only from associated basaltic rocks ( $1\text{-Gs}$ ,  $\text{Al}_2\text{O}_3/\text{TiO}_2=7$ ) but also from felsic rocks, because the cherts show considerable higher value (Fig. 8a)(Yamamoto et al., 1986). The  $\text{Al}_2\text{O}_3/\text{TiO}_2$  values for felsic rocks in the underlying Duffer Formation range

from 18 to 70 (calculated from data of Hickman (1983)). Some white and grey cherts with high values may contain a large amount of felsic debris, because they contain very little Fe-oxides that can adsorb Al.

Evaporites are uncommon in the Marble Bar Chert, whereas they have been reported to occur within several strata of the Warrawoona Group (Buick and Dunlop, 1990; Lowe, 1983). An evaporitic environment, therefore, appears not to have been common in the period of the formation of the cherts. Barley et al. (1979) suggested that the depositional basin of the Warrawoona Group was fairly flat and that vents of felsic volcanoes formed local topographic highs. Evaporites and stromatolites well-exposed within the Strelley Pool Chert (Lowe, 1983), a lateral equivalent of the Marble Bar Chert, are inferred to have been deposited in a restricted area around a topographic high or enclosed by these highs. The Marble Bar Chert, on the other hand, probably was deposited in a somewhat deeper water distant from the evaporitic region. The present grey cherts are characterised by carbonaceous materials and detrital components as described above. Such carbonaceous grey cherts are reported to occur within the Strelley Pool Chert by Lowe (1983), who considered organic-rich sediments to have been their precursors. If the grey cherts from Marble Bar and from Strelley Pool are of the same origin, an evaporitic environment favorable for the grey chert deposition may have prevailed sporadically in the Marble Bar basin, when subaerial weathering supplied detrital materials into the depository.

### *Pillow Hill*

The chert layers at Pillow Hill do not contain any Fe-rich layers ( $\text{Fe}_2\text{O}_3^* > 10\%$ ), but the positive Eu-anomaly (Fig. 7) point to the hydrothermal origin. Fe and Mn-

enrichments in rhombic carbonates (Table 4) also indicate that they were precipitated from solutions buffered by hydrothermal components (Veizer et al., 1989). Lead and Zn in the banded cherts, in this context, were probably supplied through hydrothermal activity related to the submarine volcanism that formed pillow lavas. Both elements appear to have been extracted hydrothermally from basalts (Seyfried and Mottl, 1982; Trocine and Trefry, 1988).

Based on the  $\text{Al}_2\text{O}_3/\text{TiO}_2$  values (Fig. 8a), detrital materials in the cherts from Pillow Hill are inferred to have been derived mostly from the basalts. The basal greenish-grey cherts, in particular, might be silicified basaltic ash.

### *Roebourne*

The Roebourne cherts, unlike the Marble Bar Chert, are dominated by pale yellowish-grey and grey cherts. Such pale yellowish-grey and grey cherts contain a considerable amount of clay minerals, represented by high concentrations of Al, Ti and K. The lithologic features and high  $\text{Al}_2\text{O}_3/\text{TiO}_2$  values (Table 2) suggest the possibility that pale yellowish-grey cherts are silicified acidic tuff (Yamamoto et al., 1986). The lower  $\text{Al}_2\text{O}_3/\text{TiO}_2$  value for the grey chert compared with the pale yellowish-grey cherts indicates that the former received more basaltic debris than the latter. A minor amount of laminated chert consists of alternate bands of white and black-dusty cherts, and the latter contains more Al, Ti, Fe and Zr than the former (Table 2). The banding is believed to have been caused by intermittent supply of detrital materials. These chert layers were probably deposited relatively close to land, where ash derived from the felsic and basic volcanism fell and perhaps detrital quartz was supplied as well.

### *Coppin Gap and Point Samson*

At Coppin Gap, the occurrences of conglomerate, shale and sandstone containing detrital zircon suggest that a clastic source existed close to the depositional basin. The  $\text{Al}_2\text{O}_3/\text{TiO}_2$  values in the BIFs are similar to those in the shales (Fig. 8a), which implies a common source for their detrital materials.

Red bands in the BIFs from Point Samson contain more Al, Ti, Mg, K, and Zr than the Fe-rich samples from other locations (Table 2) described above. Positive correlations of  $\text{TiO}_2$  against MgO and  $\text{K}_2\text{O}$  (Fig. 11) imply that these elements were contained in detrital materials, but the element/ $\text{TiO}_2$  values in the BIFs are different from those in the shales. The significance of the variability of  $\text{Al}_2\text{O}_3/\text{TiO}_2$  in the samples from Point Samson is not understood.

## Geochemical significance of clastic components

### *Diagenetic aspects of the shales and sandstone*

It should be noted that Archean shales and sandstone show the same trend as found in recent marine sediments from various oceanic regions on the  $\text{Al}_2\text{O}_3/\text{TiO}_2$ - $\text{K}_2\text{O}/\text{TiO}_2$  diagram (Fig. 12); the  $\text{Al}_2\text{O}_3/\text{K}_2\text{O}$  values for the clastic sediments vary within a small range (from 3 to 6). This trend, however, does not show a simple mixture of detrital materials with low  $\text{Al}_2\text{O}_3/\text{TiO}_2$  and  $\text{K}_2\text{O}/\text{TiO}_2$  and those with high  $\text{Al}_2\text{O}_3/\text{TiO}_2$  and  $\text{K}_2\text{O}/\text{TiO}_2$ , because the values of  $\text{Al}_2\text{O}_3/\text{K}_2\text{O}$  for volcanic rocks, which can be regarded as detrital sources, fluctuate widely. The values for felsic rocks in the Pilbara Block range, for example, from 1 to 28 (calculated from data of Hickman, 1983). This trend implies that authigenic clay minerals formed through common diagenetic processes such

as ion-exchange (K-uptake) between sea-water and primary clay minerals as weathering products. The diagenetic environments resulting in clay mineral-formation in the "Pilbara Ocean", therefore, could not be significantly different from those in modern oceans.

#### *Al<sub>2</sub>O<sub>3</sub>/TiO<sub>2</sub> values in the samples*

The Al<sub>2</sub>O<sub>3</sub>/TiO<sub>2</sub> values for most marine sediments are within the range of 20 to 25 (Sugisaki et al., 1982), and these sediments (enclosed by a dashed line in Fig. 12) can be regarded as well-mixed detrital materials derived from the upper crust. The values for Archean shales from the Pilbara Block, on the other hand, do not converge on a specific value. The fluctuation may reflect the variation in composition of local volcanic assemblages and the detrital sources. Shales from Point Samson with lower Al<sub>2</sub>O<sub>3</sub>/TiO<sub>2</sub> values, in comparison with those from Coppin Gap with higher values, may have been derived largely from basaltic precursors. Most shales with higher Al<sub>2</sub>O<sub>3</sub>/TiO<sub>2</sub> values from 25 to 56 reported by McLennan et al. (1983) must contain more felsic debris than those in this study (Yamamoto et al., 1986).

It should be noted that about 60% of the cherts from the Warrawoona Group have Al<sub>2</sub>O<sub>3</sub>/TiO<sub>2</sub> values between 10 and 30 (Fig. 8b). This suggests a major detrital components in the ferruginous sedimentary rocks and cherts. Even the ratios in Fe-rich samples that contain chemically scavenged Al, as described above, do not seriously disturb the overall trend. The chemical composition of very fine detritus commonly supplied into the "Pilbara Ocean" can, therefore, be assumed on the basis of detrital materials in cherts. The analytical data for Al and Ti for grey and greenish-grey cherts enriched in these elements are most reliable for the estimation of the ratio of the detrital materials. Grey and greenish-grey cherts show a positive correlation between Al<sub>2</sub>O<sub>3</sub> and TiO<sub>2</sub> (Fig. 14)

and have a ratio that ranges from 15 to 35, with an average of 20, except for two samples from Marble Bar. This average value is not remarkably different from the general trend of all samples. DiMarco and Lowe (1989) suggested that grey to greenish-grey cherts within several strata of the Warrawoona Group are derived from basic volcanic ash. The  $\text{Al}_2\text{O}_3/\text{TiO}_2$  values in grey cherts from Marble Bar, however, are much higher than those of basic volcanics as described above, and hence the grey cherts may contain felsic detritus of higher  $\text{Al}_2\text{O}_3/\text{TiO}_2$  values.  $\text{Al}_2\text{O}_3/\text{TiO}_2$  values in the samples from the Gorge Creek Group fluctuate widely (Fig. 8b). This is due for the most part to the high variability of the values in samples from Point Samson.

The chemical composition of the Archean upper crust has been discussed on the basis of chemical indicators such as La/Th and REE in shales by many authors (e.g. Jakes and Taylor, 1974; McLennan et al., 1980). In the case of the Pilbara Block, the overall composition, however, is likely to have been altered by local volcanic assemblages as discussed above. Felsic detritus probably accumulated more easily than basaltic detrital materials, because felsic volcanoes tend to form topographical highs (Lowe and Knauth, 1977). The estimated composition of the upper crust, therefore, tends to be more felsic than its true composition, even though felsic rocks are minor parts of the Archean crust. McLennan et al.'s revision (1983) of the Archean upper crust toward more felsic composition, consequently, should be critically reexamined. It seems to be uncertain in either case whether or not Archean shales can be regarded as well-mixed detrital materials derived from the Archean upper crust. The trend of  $\text{Al}_2\text{O}_3/\text{TiO}_2$  values noted in the Pilbara chert layers, on the other hand, suggests that they may provide helpful information about the upper crust in the Archean. The  $\text{Al}_2\text{O}_3/\text{TiO}_2$  value in Archean cherts can be

a clue to the crustal evolution in the early Precambrian because of minor development of clastic sediments during the period.

## Concluding Remarks

### *The volcanogenic Pilbara Ocean*

Fryer et al. (1979) suggested, on the basis of Sr-isotope and REE-patterns in BIFs and data of ore deposits, that Archean oceans had been enriched predominantly in volcanogenic components. Iron and REE in Archean BIFs were derived largely from submarine hydrothermal systems (Dymek and Klein, 1988; Jacobsen and Piementel-Klose, 1988; Derry and Jacobsen, 1990). The majority of these studies emphasise that Archean BIFs were of hydrothermal origin, although the possibility of Fe and Si in post-Archean BIFs having been derived principally from continental weathering can not be excluded (Miller and O'Nions, 1985). Geochemical characteristics of the present chert layers including ferruginous sedimentary rocks, explicitly confirm a hydrothermal origin. Ferruginous cherts are reported to occur in other chert units such as North Pole Chert (Buick and Dunlop, 1990). This confirms that the precipitation of Fe as oxides or carbonates occurred extensively in the "Pilbara Ocean". Evidently, the "Pilbara Ocean" was full of Fe and Si that was from submarine hydrothermal systems.

Hematite pseudomorphs after rhombic carbonate and possible pyrite and magnetite were abundant in some Fe-rich samples. The Fe-mineral assemblage (hematite-magnetite-siderite) in BIFs of the Dales Gorge Member, Hamersely, was interpreted as follows:  $\text{Fe}(\text{OH})_3$  as a primary solid phase of ferric iron reacted with carbon and released ferrous iron, which resulted in the formation of siderite, magnetite and possibly pyrite

(Ewers, 1983). Kimberley (1974) and Lougheed (1983), on the contrary, emphasise that iron-oxides such as hematite and magnetite in BIF are formed by oxidation of Fe-bearing carbonates (siderite and ankerite). The latter mechanism, however, is not consistent with the presence of fine hematite grains forming peloidal structures in some of the present fresh samples that are possible primary precipitates. The former mechanism described by Ewers (1983) is the most likely process for the formation of the present ferruginous sedimentary rocks. Oxidizing agents that precipitated ferrous iron as ferric oxides can not be specified. As well as oxygen, oxidizing radicals produced by photochemical reactions within the water and the atmosphere might have been responsible for the formation of the present ferric oxides (Walker et al., 1983).

Morris and Horwitz (1983) regarded the low content of detrital materials in Precambrian BIFs as evidence for their deposition on a platform or a bank where the supply of detrital materials was restricted. At Coppin Gap, however, clastic rocks such as sandstone and conglomerate alternate with BIFs and cherts that contain little detrital materials. A clastic layer containing detrital quartz, zircon and rutile occurs within the chert layer at Marble Bar. Detrital quartz grains are also found within the chert layer at Roebourne. Fe-rich deposits precipitated from mineral-springs on land also show low concentrations of Al and Ti as do the present samples (Kanai, 1989). The depletion in detrital materials in the present samples, therefore, can be attributed to rapid precipitation of Fe and Si resulting in dilution of detrital materials rather than deposition in an environment lacking detritus input.

#### *On the banding of Fe- and Si-rich layers*

Holland (1973) suggested that the banding of Si and Fe in BIFs may have resulted

from intermittent upwelling of deep-water from a reduced environment that contains significant amounts of ferrous iron into shallow and oxic water on the shelf. The BIFs in the Gorge Creek Group is supposed to have been deposited on an extensive shallow continental shelf (Hickman, 1983). The banding of BIFs from Coppin Gap and Point Samson may have been formed by an upwelling mechanism. Barley et al. (1979), on the other hand, suggested that the depositional basin of the Warrawoona Group was fairly flat, where such upwelling could not take place. The cause of banding of Fe and Si in the chert layers of the Warrawoona Group, therefore, requires some other explanations than upwelling.

#### *On the silicification of carbonates*

There has been a debate on the origin of cherts in Archean greenstone belts. Sedimentological evidence on cherts from the Onverwacht Group, South Africa, suggests that they were silicified terrigenous materials (Lowe and Knauth, 1977; Paris et al., 1985). The present samples, on the contrary, mostly lack sedimentary structures such as ripple marks, cross lamination and graded bedding. This precludes the possibility of terrigenous sediments as the precursor of most of the Pilbara cherts. Lowe and Knauth (1977) also suggested, with some uncertainties, that some of the Archean chert layers that lack sedimentary structures represent a carbonate - silica - evaporite sequence. Precipitation of amorphous silica-gel is believed to have played a dominant role in the formation of the present chert layers, even though partially or completely silicified carbonate grains were detected in some cherts under the microscope. As discussed above, the "Pilbara Ocean" appears to have been enriched in hydrothermally-derived Fe and Si.

### *Significance of the geochemical study of Archean chert*

Previous studies on Archean cherts have mostly been sedimentological, and geochemical studies of them have not been emphasised. The present study, however, shows that sedimentological and petrographical characteristics of the chert layers of the Warrawoona Group in the Pilbara Block are closely related to their chemical compositions: (1) Red cherts containing hematite generally show high concentrations of  $\text{Fe}_2\text{O}_3^*$ , and heavy metals such as Ni and Zn may have been coprecipitated with Fe-oxides; (2) Concentrations of  $\text{Fe}_2\text{O}_3^*$  in some red cherts are higher than 10%, and their chemical characteristics such as low heavy metal concentrations, low  $\text{MnO}/\text{Fe}_2\text{O}_3^*$  values, low Ni/Zn and Co/Zn values and REE patterns showing positive Eu-anomalies, indicate hydrothermal origin; (3) Grey, greenish-grey and pale yellowish-grey cherts containing significant amounts of clay minerals are enriched in Al and Ti, which shows considerable contribution of detrital materials, whereas red and white cherts are characteristic of low concentrations of Al and Ti.

The results of this study emphasise the significance of geochemical study of Archean cherts. They are composed mostly of Si and/or Fe; nevertheless, the detailed analyses provide valuable information for their origin. In particular,  $\text{Al}_2\text{O}_3/\text{TiO}_2$  values in grey, greenish-grey and pale yellowish-grey cherts are indicators of an abundance of detrital materials contained in the cherts, which may also be indicative of the composition of the upper crust in the Archean. Concentrations of heavy metals such as Ni, Zn and Pb probably reflect hydrothermal contributions. Geochemical studies on Archean cherts, coupled with sedimentological and petrographical studies, could provide an indication of the chemical evolution of the atmosphere, ocean and upper crust during an early history

of the Earth.

## Acknowledgement

I thank the members of the Department of Earth Sciences, Nagoya University. I especially wish to express my gratitude to Professor. R. Sugisaki, who continually gave me suggestions and criticism; to Dr. M. Adachi, who gave help and constructive suggestions; to Dr. K. Suzuki, who gave advice on microprobe analyses; to Mr. S. Yogo, who prepared thin sections for all samples. I am further indebted to Mrs. K. Taki, Dr. K. Nagamine, Miss M. Tamai and Mr. Y. Horiuchi for their technical assistance and encouragement. I gratefully acknowledge my parents who always encouraged me in my studies.

## References

- Adachi, M., Yamamoto, K. and Sugisaki, R., 1986. Hydrothermal chert and associated siliceous rocks from the northern Pacific: Their geological significance as indication of ocean ridge activity. *Sediment. Geol.*, 47: 125-148.
- Balistreri, L.S. and Murray, J.W., 1982. The adsorption of Cu, Pb, Zn, and Cd on goethite from major ion seawater. *Geochim. Cosmochim. Acta*, 46: 1253-1265.
- Barley, M.E., Dunlop, J.S.R., Glover, J.E. and Groves, D.I., 1979. Sedimentary evidence for an Archaean shallow-water volcanic-sedimentary facies, eastern Pilbara Block, Western Australia. *Earth Planet. Sci. Lett.*, 43: 74-84.
- Baturin, G.N., 1988. The Geochemistry of manganese and manganese nodules in the ocean. D. Reidel, Dordrecht, 136 pp.
- Beukes, N.J. and Klein, C., 1990. Geochemistry and sedimentology of a facies transition -from microbanded to granular iron-formation- in the early Proterozoic Transvaal Supergroup, South Africa. *Precambrian Res.*, 47: 99-139.
- Boström, K. and Widenfalk, L., 1984. The origin of iron-rich muds at the Kameni Islands, Santorini, Greece. *Chem. Geol.*, 42: 203-218.
- Buick, R. and Dunlop, J.S.R., 1990. Evaporitic sediments of Early Archaean age from the Warrawoona Group, North Pole, Western Australia. *Sedimentology*, 37: 247-277.

- Canadian American Seamount Expedition, 1985. Hydrothermal vents on an axis seamount of the Juan de Fuca ridge. *Nature*, 313: 212-214.
- Corliss, J.B., Lyle, M., Dymond, J. and Crane, K., 1978. The chemistry of hydrothermal mounds near the Galapagos Rift. *Earth Planet. Sci. Lett.*, 40: 12-24.
- Derry, L.A. and Jacobsen, S.B., 1990. The chemical evolution of Precambrian seawater: Evidence from REEs in banded iron formations. *Geochim. Cosmochim. Acta*, 54: 2965-2977.
- DiMarco, M.J. and Lowe, D.R., 1989. Stratigraphy and sedimentology of an early Archean felsic volcanic sequence, eastern Pilbara Block, Western Australia, with special reference to the Duffer Formation and implications for crustal evolution. *Precambrian Res.*, 44: 147-169.
- Duchač, K.C. and Hanor, J.S., 1987. Origin and timing of the metasomatic silicification of an early Archean komatiite sequence, Barberton Mountain Land, South Africa. *Precambrian Res.*, 37: 125-146.
- Dymek, R.F. and Klein, C., 1988. Chemistry, petrology and origin of banded iron-formation lithologies from the 3800 Ma Isua Supracrustal Belt, West Greenland. *Precambrian Res.*, 39: 247-302.
- Ewers, W.E., 1983. Chemical factors in the deposition and diagenesis of banded iron-formation. In: A.F. Trendall and R.C. Morris (Editors), *Iron-formation: Facts and Problems*, Elsevier, Amsterdam, pp.491-512.
- Ewers, W.E. and Morris, R.C., 1981. Studies of the Dales Gorge Member of the Brockman Iron Formation, Western Australia. *Econ. Geol.*, 76: 1929-1953.
- Fryer, B.J., 1983. Rare earth elements in iron-formation. In: A.F. Trendall and R.C.

- Morris (Editors), Iron-formation: Facts and Problems, Elsevier, Amsterdam, pp.345-358.
- Fryer, B.J., Fyfe, W.S. and Kerrich, R., 1979. Archaean volcanogenic oceans. *Chem. Geol.*, 24: 25-33.
- Gole, M.J., 1981. Archean banded iron-formations, Yilgarn Block, Western Australia. *Econ. Geol.*, 76: 1954-1974.
- Gole, M.J. and Klein, C., 1981. Banded iron-formations through much of Precambrian time. *Jour. Geol.*, 89: 169-183.
- Grill, E.V. and Chase, R.L., MacDonald R.D. and Murray J.W., 1981. A hydrothermal deposit from Explorer Ridge in the northeast Pacific Ocean. *Earth Planet. Sci. Lett.*, 52: 142-150.
- Gross, G.A. and McLeod, C.R., 1980. A preliminary assessment of the chemical composition of iron formations in Canada. *Canadian Mineral.*, 18: 223-229.
- Haymon, R.M. and Kastner, M., 1981. Hot spring deposits on the East Pacific Rise at 21°N: preliminary description of mineralogy and genesis. *Earth Planet. Sci. Lett.*, 53: 363-381.
- Herzig, P.M., Becker, K.P., Stoffers, P., Bäcker, H. and Blum, N., 1988. Hydrothermal silica chimney fields in the Galapagos Spreading Center at 86°W. *Earth Planet. Sci. Lett.*, 89: 261-272.
- Hickman A.H., 1983: Geology of the Pilbara Block and its environs. *West. Australia Geol. Survey Bull.* 127.
- Holland, H.D., 1973. The oceans: A possible source of iron in iron-formations. *Econ. Geol.*, 68: 1169-1172.

- Jacobsen, S.B. and Pimentel-Klose, M.R., 1988. A Nd isotopic study of the Hamersley and Michipicoten banded iron formations: the source of REE and Fe in Archean oceans. *Earth Planet. Sci. Lett.*, 87: 29-44.
- Jakes, P. and Taylor, S.R., 1974. Excess europium content in Precambrian sedimentary rocks and continental evolution. *Geochim. Cosmochim. Acta*, 38: 739-745.
- Kanai, Y., 1989. Chemical composition of the spring deposits from the Masutomi spring, Yamanashi Prefecture. *Chikyukagaku*, 23: 77-83.
- Kimberley, M.M., 1974. Origin of iron ore by diagenetic replacement of calcareous oolite. *Nature*, 250: 319-320.
- Lougheed, M.S., 1983. Origin of Precambrian iron-formations in the Lake Superior region. *Geol. Soc. Am. Bull.*, 94: 325-340.
- Lövgren, L., Sjöberg, S. and Schindler, P.W., 1990. Acid/base reactions and Al(III) complexation at the surface of goethite. *Geochim. Cosmochim. Acta*, 54: 1301-1306.
- Lowe, D.R., 1983. Restricted shallow-water sedimentation of Early Archean stromatolitic and evaporitic strata of the Strelley Pool Chert, Pilbara Block, Western Australia. *Precambrian Res.*, 19: 239-283.
- Lowe, D.R. and Knauth, L.P., 1977. Sedimentology of the Onverwacht Group (3.4 billion years), Transvaal, South Africa, and its bearing on the characteristics and evolution of the early earth. *Jour. Geol.*, 85: 699-723.
- Marchig, V., Gundlach, H., Moller, P. and Schley, F., 1982. Some geochemical indicators for discrimination between diagenetic and hydrothermal metalliferous sediments. *Mar. Geol.*, 50: 241-256.

- McLennan, S.M., Nance, W.B. and Taylor, S.R., 1980. Rare earth element-thorium correlations in sedimentary rocks, and the composition of the continental crust. *Geochim. Cosmochim. Acta*, 44: 1833-1839.
- McLennan, S.M., Taylor, S.R. and Eriksson, K.A., 1983. Geochemistry of Archean shales from the Pilbara Supergroup, Western Australia. *Geochim. Cosmochim. Acta*, 47: 1211-1222.
- Miller, R.G. and O'Nions, R.K., 1985. Source of Precambrian chemical and clastic sediments. *Nature*, 314: 325-330.
- Morris, R.C. and Horwitz, R.C., 1983. The origin of the iron-formation-rich Hamersley Group of Western Australia - deposition on a platform. *Precambrian Res.*, 21: 273-297.
- Oversby, V.M., 1976. Isotopic ages and geochemistry of Archaean acid igneous rocks from the Pilbara, Western Australia. *Geochim. Cosmochim. Acta*, 40: 817-829.
- Paris, I., Stanistreet, I.G. and Hughes, M.J., 1985. Cherts of the Barberton greenstone belt interpreted as products of submarine exhalative activity. *Jour. Geol.*, 93: 111-129.
- Pidgeon, R.T., 1978. 3450-m.y.-old volcanics in the Archaean layered greenstone succession of the Pilbara Block, Western Australia. *Earth Planet. Sci. Lett.*, 37: 421-428.
- Robertson, A.H.F. and Hudson, J.D., 1973. Cyprus umbers: Chemical precipitates on a Tethyan ocean ridge. *Earth Planet. Sci. Lett.*, 18: 93-101.
- Seyfried, W.E.Jr. and Mottl, M.J., 1982. Hydrothermal alteration of basalt by seawater under seawater-dominated conditions. *Geochim. Cosmochim. Acta*, 46: 985-

1002.

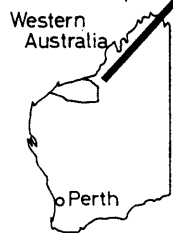
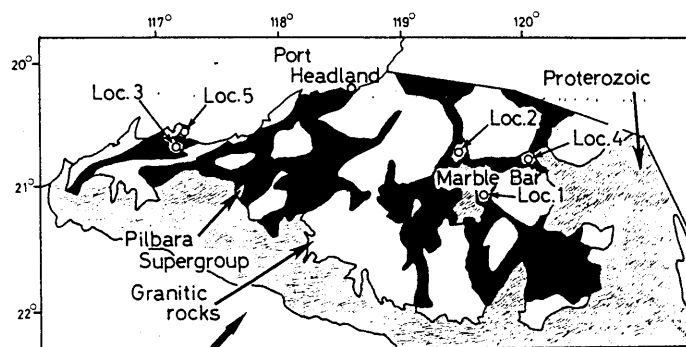
- Stiers, W. and Schwertmann, U., 1985. Evidence for manganese substitution in synthetic goethite. *Geochim. Cosmochim. Acta*, 49: 1909-1911.
- Sugisaki, R., 1978. Chemical composition of argillaceous sediments on the Pacific margin of southwest Japan. In: E. Inoue (Editor) *Geol. Surv. Japan Cruise Rep.*, 9: 65-73.
- Sugisaki, R., 1979. Chemical composition of argillaceous sediments around the Yamato Bank in the Japan sea. In: E. Honza (Editor) *Geol. Surv. Japan Cruise Rep.*, 13: 75-88.
- Sugisaki, R., 1981. A modified method of analysis of bulk chemical composition of argillaceous sediments and data display with special reference to marine sediments. *J. Geol. Soc. Jpn.*, 87: 77-85.
- Sugisaki, R. and Kinoshita, T., 1981. Chemical composition of marine argillaceous sediments around the Izu-Ogasawara Islands. In: E. Honza et al. (Editors) *Geol. Surv. Japan Cruise Rep.*, 14: 146-158.
- Sugisaki, R. and Kinoshita, T., 1982. Major element chemistry of the sediments on the central Pacific transect, Wake to Tahiti, GH80-1 cruise. In: A. Mizuno and S. Nakao (Editors) *Geol. Surv. Japan Cruise Rep.*, 18: 293-312.
- Sugisaki, R., Kinoshita, T., Shimomura, T. and Ando, K., 1981. An automatic X-ray fluorescence method for the trace element analyses in silicate rocks. *J. Geol. Soc. Jpn.*, 87: 675-688.
- Sugisaki, R., Shimomura, T. and Ando, K., 1977. An automatic X-ray fluorescence method for the analysis of silicate rocks. *J. Geol. Soc. Jpn.*, 83: 725-733.

- Sugisaki, R., Yamamoto, K. and Adachi, M., 1982. Triassic bedded cherts in central Japan are not pelagic. *Nature*, 298: 644-647.
- Sugitani, K., Sano, H., Adachi, M. and Sugisaki, R., 1991. Permian hydrothermal deposits in the Mino Terrane, central Japan: implications for hydrothermal plumes in an ancient ocean basin. *Sediment. Geol.*, 71: 59-71.
- Toth, J.R., 1980. Deposition of submarine crusts rich in manganese and iron. *Geol. Soc. Am. Bull.*, 91: 44-54.
- Trocine, R.P. and Trefry, J.H., 1988. Distribution and chemistry of suspended particles from an active hydrothermal vent site on the Mid-Atlantic Ridge at 26°N. *Earth Planet. Sci. Lett.*, 88: 1-15.
- Varnavas, S.P. and Panagos, A.G., 1984. Mesozoic metalliferous sediments from the ophiolites of Ermioni, Greece; analogue to Recent mid-ocean ridge ferromanganese deposits. *Chem. Geol.*, 42: 227-242.
- Veizer, J., Hoefs, J., Lowe, D.R., and Thurston, P.C., 1989. Geochemistry of Precambrian carbonates: II. Archean greenstone belts and Archean sea water. *Geochim. Cosmochim. Acta*, 53: 859-871.
- Walker, J.C.G., Klein, C., Schidlowski, M., Schopf, J.W., Stevenson, D.J. and Walter M.R., 1983. Environmental evolution of the Archean-early Proterozoic earth. In: J.W. Schopf (Editor), *Earth's earliest biosphere*, Princeton University Press, pp.260-290.
- Yamamoto, K., 1983. Geochemical study of Triassic bedded cherts from Kamiasso, Gifu Prefecture. *J. Geol. Soc. Jpn.*, 89: 143-162.
- Yamamoto, K., 1987. Geochemical characteristics and depositional environments of cherts

and associated rocks in the Franciscan and Shimanto Terranes. *Sediment. Geol.*, 52: 65-108.

Yamamoto, K. and Sugisaki, R., 1986. Geochemical characteristics of deep-sea sediments around 3°N, 169°W, the Pacific Ocean: samples for GH81-4 cruise, Geological Survey of Japan. In: S. Nakao (Editor) *Geol. Surv. Japan Cruise Rep.*, 21: 195-208.

Yamamoto, K., Sugisaki, R. and Arai, F., 1986. Chemical aspects of alteration of acidic tuffs and their application to siliceous deposits. *Chem. Geol.*, 55: 61-76.



- Loc. 1 Marble Bar
- Loc. 2 Pillow Hill
- Loc. 3 Roebourne
- Loc. 4 Coppin Gap
- Loc. 5 Point Samson

Fig. 1

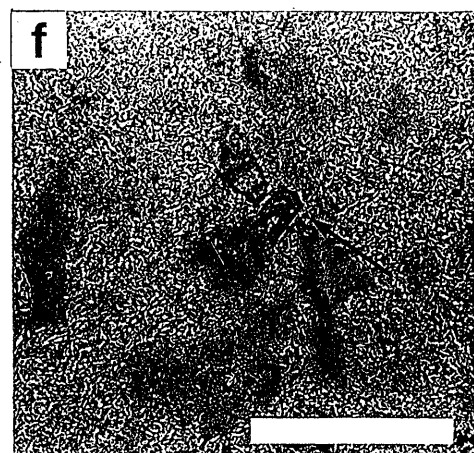
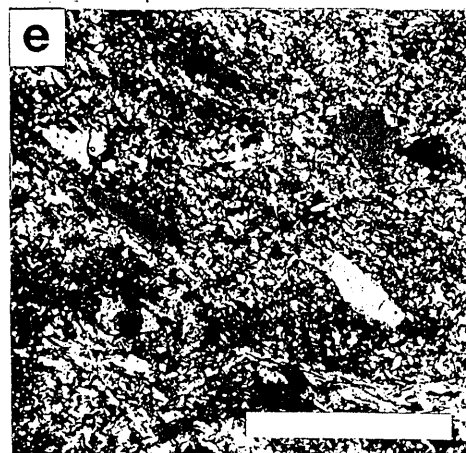
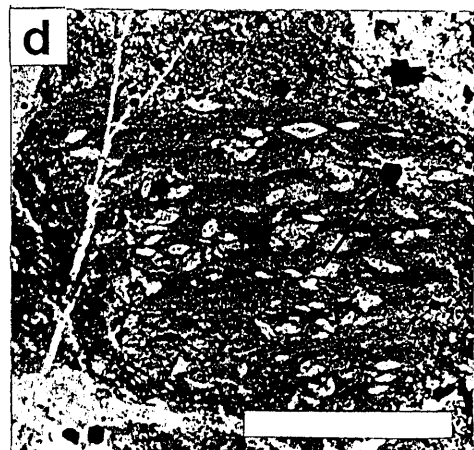
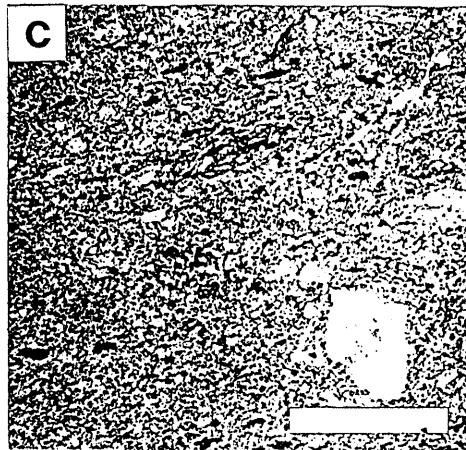
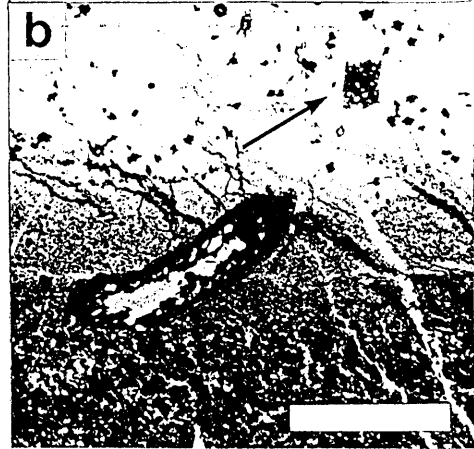
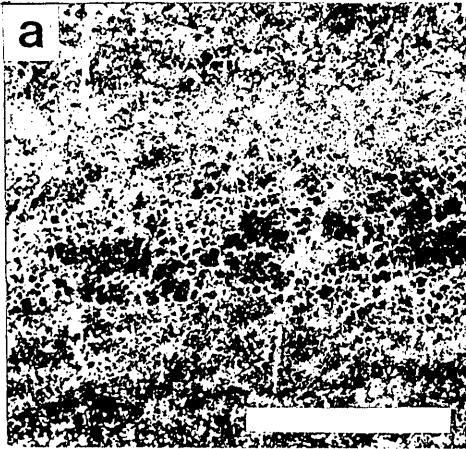


Fig. 2

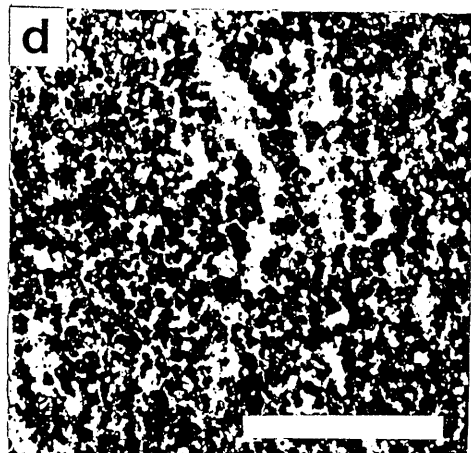
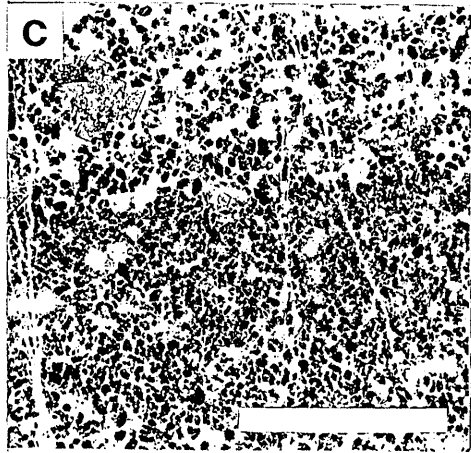
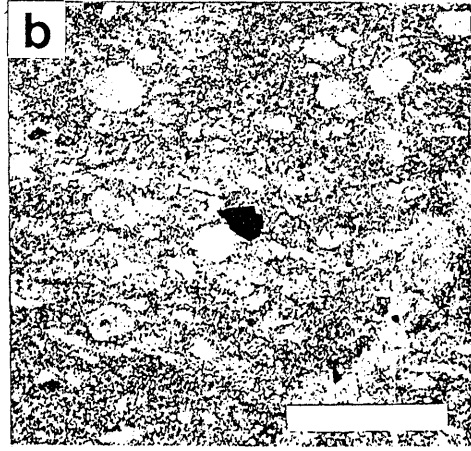
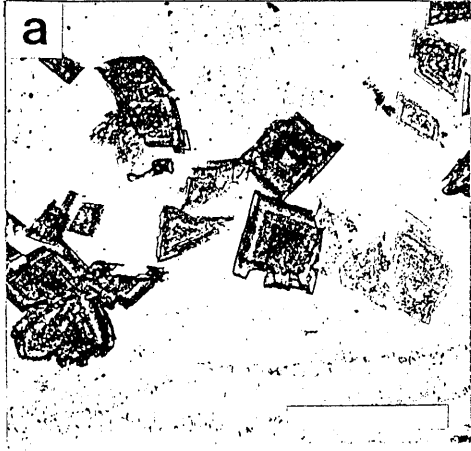


Fig. 3

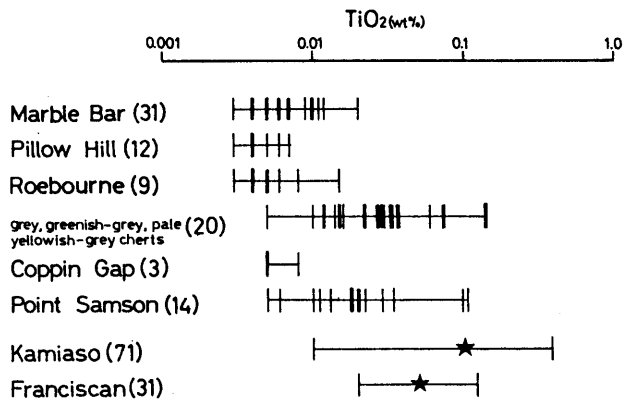


Fig. 4

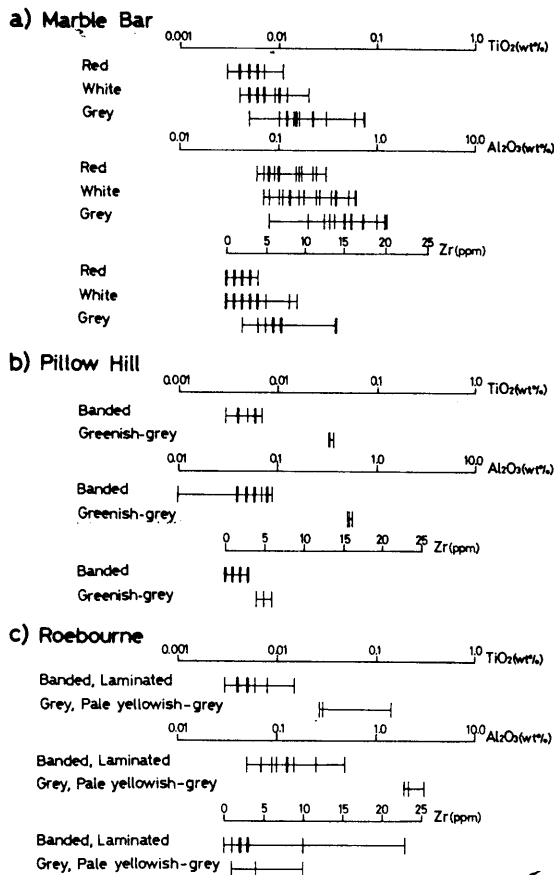


Fig. 5

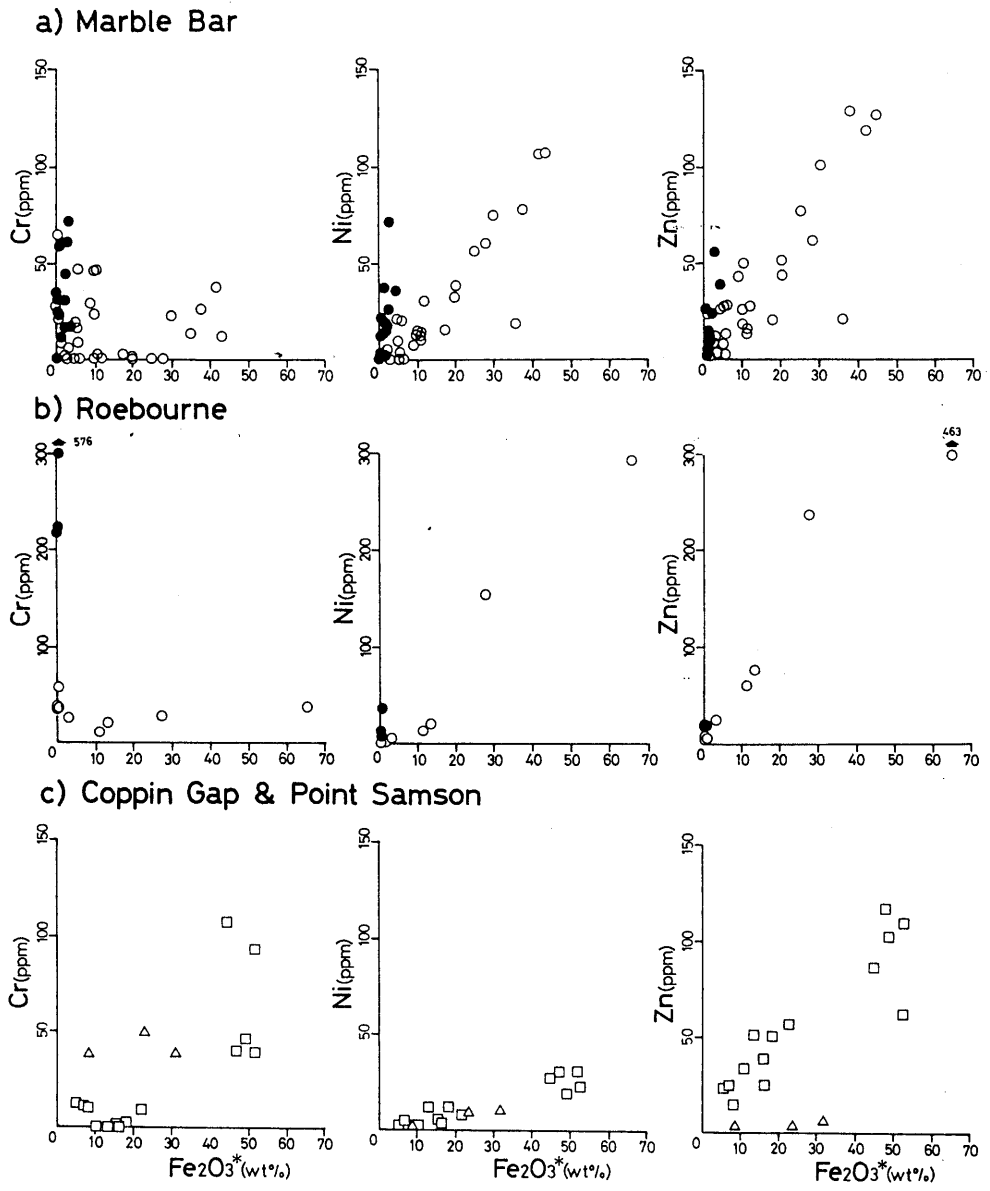


Fig. 6

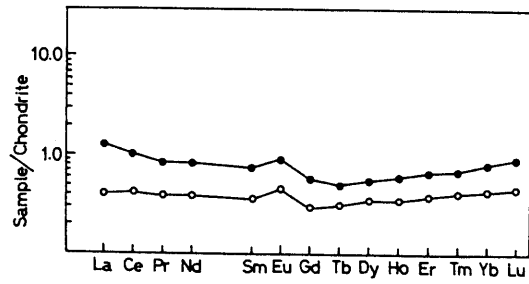


Fig. 7

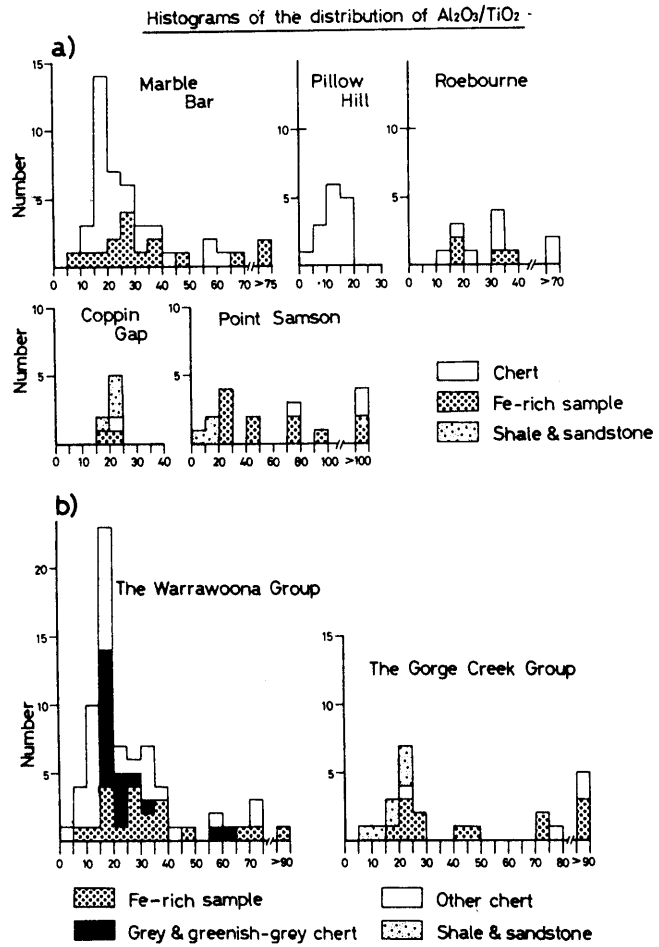


Fig. 8

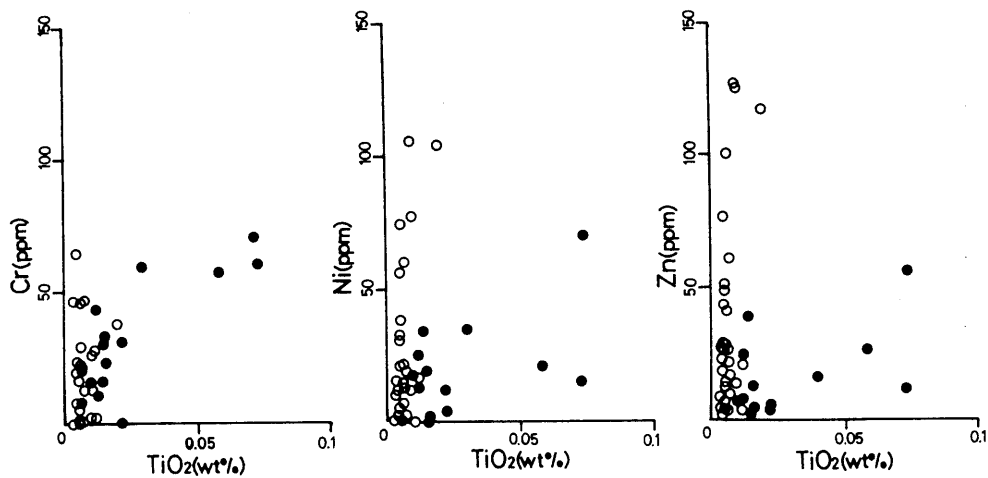


Fig. 9

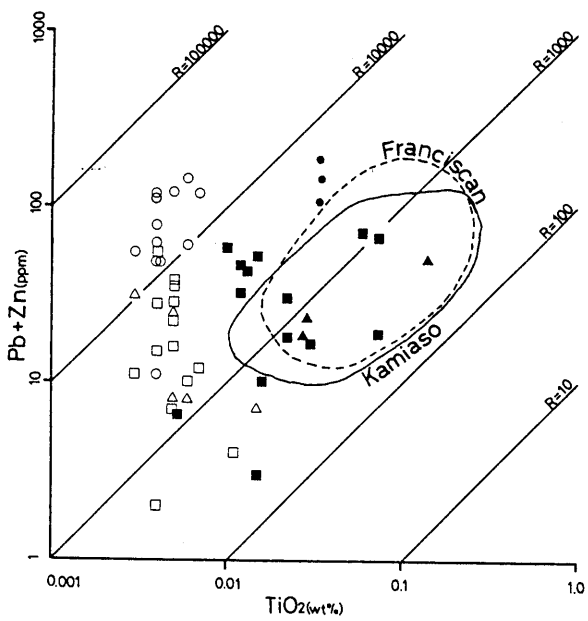


Fig. 10

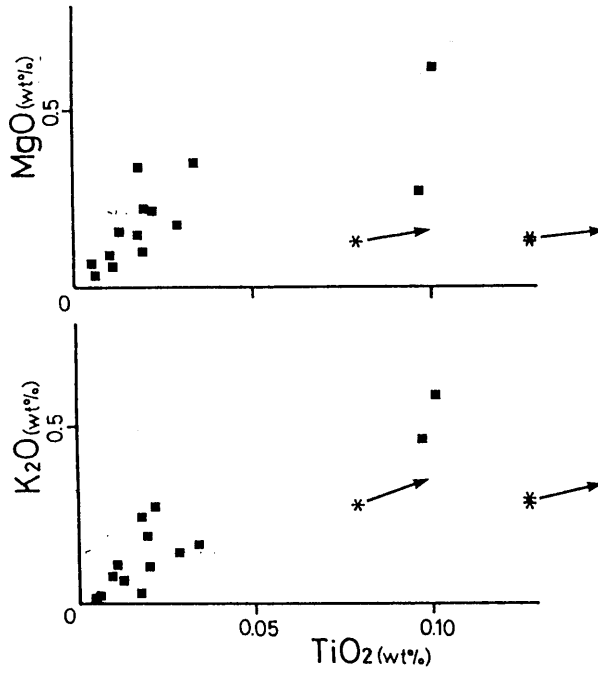


Fig. 11

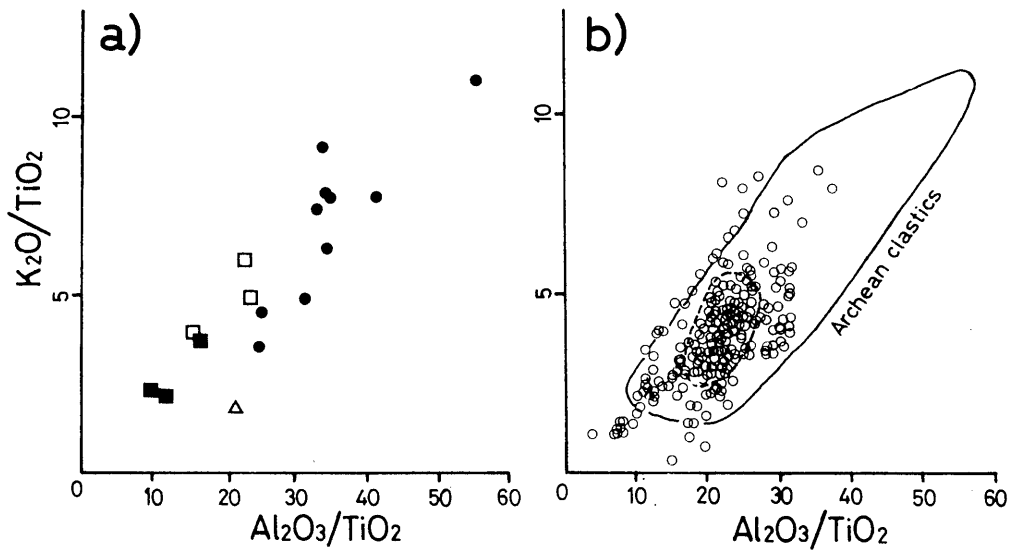


Fig. 12

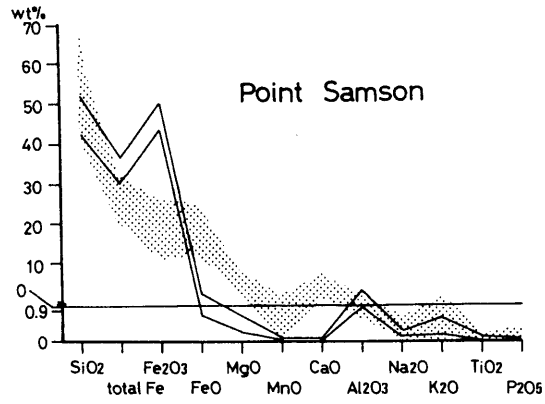
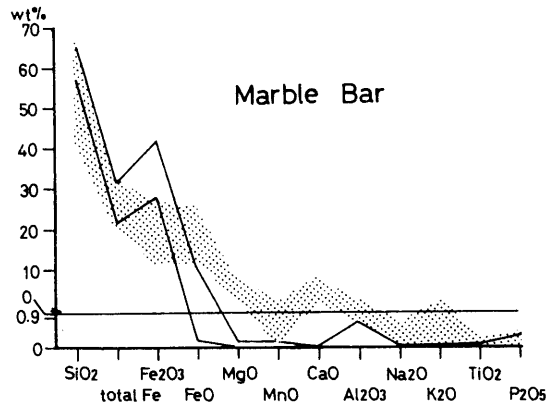


Fig. 13

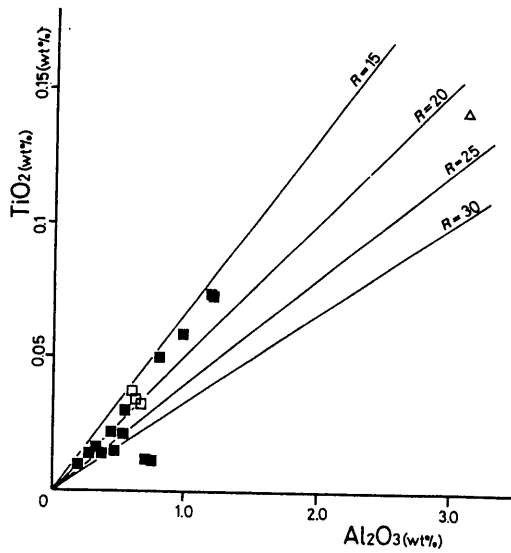


Fig. 14

Fig. 1 Sample locations of Archean sedimentary rocks in the Pilbara Block. The simplified-geological map is drawn after Hickman (1983).

Fig. 2 Photomicrographs of the Marble Bar Chert. a) Fine hematite grains forming peloidal structure in a red chert. Scale bar is  $500\mu\text{m}$ . b) Hematite pseudomorph after a possible evaporite crystal (gypsum or anhydrite)(central left) at the boundary between a red band (the lower half of the photograph) and white one (the upper half) of a red-white banded chert. Hematite pseudomorph after rhombic carbonate is shown by arrow. Scale bar is 1mm. c) Carbonaceous aggregates (black) in a grey chert. Scale bar is 1mm. d) Lenticular gypsum ghosts in a grey chert. The arrow indicates a pyrite grain. Scale bar is  $500\mu\text{m}$ . e) Clastic layer containing detrital quartz and sericite in a light-grey chert. Scale bar is 1mm. f) Detrital zircon (arrow) in the clastic layer. Scale bar is  $200\mu\text{m}$ .

Fig. 3 Photomicrographs of cherts from Pillow Hill and Roebourne. a) Rhombic carbonate grains in a red-white banded chert from Pillow Hill. Scale bar is 1mm. b) Greenish-grey chert from Pillow Hill. The opaque mineral (in the center) is pyrite. Scale bar is 1mm. c) Fine hematite grains forming peloidal structure in a red-white-grey banded chert from Pillow Hill. Scale bar is  $500\mu\text{m}$ . d) Banded cherts from Roebourne. Opaque minerals are hematite and magnetite. Scale bar is 1mm.

Fig. 4  $\text{TiO}_2$  contents of the present samples except for clastic sediments from the Pilbara Block. Numerals in parentheses indicate numbers of analysed samples. Also given are those for Triassic Kamiaso biogenic chert (Yamamoto, 1983) and

Triassic Franciscan hydrothermal chert (basal 10m) (Yamamoto, 1987); average  $\text{TiO}_2$  contents are shown by stars. A thick vertical line contains several samples with the identical  $\text{TiO}_2$  content.

Fig. 5 Contents of  $\text{TiO}_2$ ,  $\text{Al}_2\text{O}_3$  and Zr in cherts from the Warrawoona Group. Lithologies are referred to Table 1. A thick vertical line contains several samples with the identical value.

Fig. 6 Plots of Cr, Ni and Zn against  $\text{Fe}_2\text{O}_3^*$  for samples, except for the Pillow Hill samples and clastic sediments from Coppin Gap and Point Samson. Solid circles show grey and pale yellowish grey cherts. Open circles show other cherts. Open squares and triangles show samples from Point Samson and Coppin Gap, respectively.

Fig. 7 Chondrite-normalized REE-patterns for red cherts from Marble Bar (1-B10, solid circle) and Pillow Hill (2-B10, open circle).

Fig. 8 Histograms of  $\text{Al}_2\text{O}_3/\text{TiO}_2$  values for all samples analysed. Fe-rich samples include Fe-rich cherts and BIFs with  $\text{Fe}_2\text{O}_3^*$  more than 10%. a) The histograms for each location. Note that the scale for samples from Point Samson is different from those for others. b) The histograms for each group.

Fig. 9 Plots of Cr, Ni and Zn against  $\text{TiO}_2$  for samples from Marble Bar. Open circles and solid ones show red-white banded cherts and grey ones, respectively.

Fig. 10 The relationship between Pb+Zn and  $\text{TiO}_2$  for cherts ( $\text{Fe}_2\text{O}_3^* < 10\%$ ) from the Warrawoona Group. Open and solid squares show white cherts and grey cherts from Marble Bar, respectively. Solid triangles show grey and pale yellowish-grey cherts and open triangles do other cherts from Roebourne.

Open and solid circles show red-white-grey banded cherts and greenish-grey cherts from Pillow Hill, respectively. R indicates the value of  $Pb+Zn/TiO_2$  shown by the line. Data for Kamiaso biogenic chert and Franciscan hydrothermal chert are quoted from Yamamoto (1983) and Yamamoto (1987), respectively.

Fig. 11 Plots of  $K_2O$  and  $MgO$  against  $TiO_2$  for samples from Point Samson. Solid squares and asterisks show BIF samples and shales, respectively.

Fig. 12 The relationship between  $Al_2O_3/TiO_2$  and  $K_2O/TiO_2$  for shales and sandstones from the Pilbara Block (a) and recent marine sediments from various regions (b). (a) Open squares and open triangle show silty shales and sandstone from Coppin Gap, respectively. Solid squares show shales from Point Samson. Solid circles show shales in the Pilbara Block studied by McLennan et al. (1983). (b) Marine sediments for reference were collected from the Central Pacific (Sugisaki and Kinoshita (1982) and Yamamoto and Sugisaki (1986)), the Izu-Ogasawara Islands (Sugisaki and Kinoshita, 1981), the Nankai Trough (Sugisaki, 1978) and the Japan Sea (Sugisaki, 1979). Distribution area for typical marine sediments as well-mixed detrital materials is encircled by dashed line.

Fig. 13 Plots of bulk chemical compositions of Fe-rich samples ( $Fe_2O_3^* > 30\%$ ) (after Gole and Klein (1981)). The dotted area shows the range of BIFs studied by Gole and Klein (1981) and Dymek and Klein (1988).

Fig. 14 The relationship between  $Al_2O_3$  and  $TiO_2$  for grey and greenish-grey cherts of the Warrawoona Group. Solid and open squares show samples from Marble

Bar and Pillow Hill, respectively. Open triangle shows a grey chert from Roebourne. R indicates the value of  $\text{Al}_2\text{O}_3/\text{TiO}_2$  shown by the line.

TABLE 1

Lithologies of sedimentary rocks studied here

---

The Warrawoona Group

Marble Bar (Loc. 1)	Towers F.	red-white-grey banded chert
Pillow Hill (Loc. 2)	Euro Basalt	red-white-grey banded chert, greenish-grey chert, tuffaceous chert
Roebourne (Loc. 3)	Towers F.	pale yellowish-grey chert, grey chert, white chert, banded chert, laminated chert

## The Gorge Creek Group

Coppin Gap (Loc. 4)	Cleaverville F.	chert*, BIF, shale, sandstone, conglomerate
Point Samson (Loc. 5)	Cleaverville F.	chert*, BIF, shale

---

Note: \* not subdivided. Location numbers are shown in Fig. 1

TABLE 2

## Bulk chemical compositions of samples from the Pilbara Block

sample	1-B1	1-B2	1-B3	1-B4	1-B5	1-B6	1-B7	1-B8	1-B9	1-B10	1-B11	1-B12	1-B13	1-B14	1-B15
SiO <sub>2</sub> (wt%)	96.31	97.35	96.38	92.45	91.93	95.17	95.90	94.54	96.15	91.95	95.91	93.62	90.46	92.44	88.27
TiO <sub>2</sub>	0.004	0.011	0.004	0.005	0.003	0.005	0.006	0.004	0.005	0.005	0.007	0.004	0.005	0.005	0.006
Al <sub>2</sub> O <sub>3</sub>	0.08	0.30	0.24	0.22	0.10	0.08	0.15	0.07	0.06	0.09	0.17	0.16	0.08	0.10	0.08
FeO	0.20	0.02	0.15	0.12	1.22	0.35	0.28	1.33	2.52	2.15	2.25	4.20	1.94	1.61	0.52
Fe <sub>2</sub> O <sub>3</sub>	0.55	0.04	0.27	3.54	3.88	1.07	0.48	4.31	-	2.52	0.12	0.49	3.96	3.78	8.18
Fe <sub>2</sub> O <sub>3</sub> *	0.77	0.06	0.44	3.67	5.23	1.46	0.79	5.79	2.80	4.91	2.62	5.15	6.11	5.57	8.76
MnO	-	-	-	-	-	-	-	-	0.03	0.10	0.51	0.09	0.11	0.07	0.03
MgO	0.01	0.01	0.01	0.02	0.02	0.02	-	0.25	0.08	0.08	0.08	0.09	0.08	0.08	0.03
CaO	-	-	-	-	-	-	-	0.03	0.03	0.04	0.03	0.03	0.04	0.05	-
Na <sub>2</sub> O	0.01	0.01	0.01	-	0.01	0.02	0.01	-	0.11	0.09	-	0.02	0.06	-	0.01
K <sub>2</sub> O	-	0.02	-	0.01	-	-	-	0.02	0.04	0.03	0.03	0.03	0.02	0.03	-
P <sub>2</sub> O <sub>5</sub>	-	-	0.01	0.02	0.02	-	0.01	0.02	0.02	0.02	0.01	0.04	0.03	0.05	0.01
H <sub>2</sub> O	0.12	0.08	0.19	0.42	0.41	0.31	0.23	0.11	0.26	1.52	0.51	0.75	0.76	1.49	1.13
CO <sub>2</sub>	-	-	-	-	-	-	-	-	-	-	-	-	-	-	0.35
Res.	0.10	0.43	0.79	0.48	0.12	0.40	0.51	-	-	-	-	-	2.33	-	-
Fe <sub>2</sub> O <sub>3</sub> /FeO	2.8	2.0	1.8	29.5	3.2	3.1	1.7	3.2	<	1.2	0.1	0.1	2.0	2.3	15.7
MnO/Fe <sub>2</sub> O <sub>3</sub> *	<	<	<	<	<	<	<	<	0.01	0.02	0.19	0.02	0.02	0.01	<
Al <sub>2</sub> O <sub>3</sub> /TiO <sub>2</sub>	20	27	60	44	33	16	25	18	12	18	24	40	16	20	13
Cr (ppm)	24	27	64	5	46	8	20	8	0	0	1	19	0	16	29
Co	2	1	0	1	1	1	1	1	3	4	2	3	6	0	2
Ni	0	0	0	1	1	0	0	0	5	21	3	10	21	3	7
Cu	0	0	0	0	6	0	0	23	120	72	33	42	39	36	11
Zn	24	4	2	4	9	7	4	4	13	27	10	28	29	14	43
Y	4	6	5	6	6	4	5	5	8	11	5	6	8	6	5
Zr	3	4	2	3	3	1	3	1	0	0	2	1	1	0	2
Nb	2	1	4	3	4	6	3	6	7	4	6	6	5	4	0
Pb	31	0	0	3	2	9	6	11	25	9	2	1	0	9	41

sample	1-B16	1-B17	1-B18	1-B19	1-B20	1-B21	1-B22	1-B23	1-B24	1-B25	1-B26	1-B27	1-B28	1-B29	1-B30
SiO <sub>2</sub> (wt%)	86.17	84.67	85.98	87.13	85.92	88.05	81.03	76.86	70.67	74.08	77.78	55.47	61.93	58.28	64.62
TiO <sub>2</sub>	0.005	0.007	0.006	0.004	0.005	0.009	0.012	0.005	0.007	0.005	0.005	0.020	0.007	0.010	0.006
Al <sub>2</sub> O <sub>3</sub>	0.07	0.26	0.13	0.38	0.16	0.24	0.59	0.34	0.18	0.13	0.10	0.60	0.51	0.38	0.11
FeO	1.15	2.51	0.49	4.55	2.79	7.98	10.01	3.65	7.07	3.65	3.87	0.21	1.25	1.02	1.11
Fe <sub>2</sub> O <sub>3</sub>	8.86	8.27	9.43	5.26	8.85	2.03	6.40	16.07	20.38	21.28	15.49	41.32	34.07	36.11	28.22
Fe <sub>2</sub> O <sub>3</sub> *	10.14	11.06	9.97	10.31	11.95	10.89	17.51	20.12	28.22	25.33	19.79	41.55	35.46	37.24	30.11
MnO	0.03	0.02	0.03	-	0.55	0.06	0.09	0.38	0.23	0.39	0.12	0.06	0.01	0.07	0.06
MgO	0.06	0.05	0.06	0.08	0.09	0.08	0.08	0.09	0.08	0.09	0.10	0.03	0.04	0.05	0.14
CaO	-	-	-	0.03	0.04	0.03	0.04	0.03	0.04	0.03	0.05	0.01	-	-	-
Na <sub>2</sub> O	-	-	0.03	0.18	0.13	0.73	-	0.22	0.25	-	-	0.05	-	-	0.02
K <sub>2</sub> O	-	-	-	0.10	0.03	0.02	0.03	0.08	0.02	0.03	0.02	-	-	-	-
P <sub>2</sub> O <sub>5</sub>	0.02	0.02	0.03	0.01	0.03	0.04	0.04	0.03	0.04	0.03	0.07	0.03	0.14	0.14	0.03
H <sub>2</sub> O	0.91	0.68	0.87	0.09	0.15	0.40	0.89	1.41	1.19	1.10	2.45	1.97	1.32	2.76	3.21
CO <sub>2</sub>	-	0.58	-	-	-	-	-	-	-	-	-	-	0.61	0.42	0.50
Res.	0.61	0.26	0.70	0.64	1.28	0.44	0.62	0.90	-	-	0.55	0.71	0.48	1.29	0.57
Fe <sub>2</sub> O <sub>3</sub> /FeO	7.7	3.3	19.2	1.2	3.2	0.3	0.6	4.4	2.9	5.8	4.0	197.8	27.3	35.4	25.4
MnO/Fe <sub>2</sub> O <sub>3</sub> *	<	<	<	<	0.05	0.01	0.01	0.02	0.01	0.02	0.01	<	<	<	<
Al <sub>2</sub> O <sub>3</sub> /TiO <sub>2</sub>	14	37	22	95	32	27	49	68	26	26	20	30	73	38	18
Cr (ppm)	23	46	45	0	0	2	2	0	0	0	1	37	13	26	22
Co	4	1	4	3	5	2	2	4	8	11	4	10	2	14	16
Ni	11	13	14	15	31	12	16	38	60	56	33	104	19	77	74
Cu	18	18	18	72	77	56	52	129	115	74	73	54	53	66	47
Zn	50	17	26	19	28	14	21	52	62	77	44	118	22	128	101
Y	4	14	8	9	10	6	11	11	15	11	10	18	13	23	10
Zr	3	0	4	1	2	3	4	1	0	0	0	8	5	9	2
Nb	4	4	5	5	5	9	6	8	5	6	6	0	5	3	2
Pb	30	5	9	0	13	3	12	6	3	8	10	126	17	23	20

sample	1-B31	1-G1	1-G2	1-G3	1-G4	1-G5	1-G6	1-G7	1-G8	1-G9	1-G10	1-G11	1-G12	1-G13	1-G14
SiO <sub>2</sub> (wt%)	50.99	96.08	95.46	95.22	94.17	94.16	95.45	95.68	94.21	90.46	93.14	94.09	97.55	90.87	98.07
TiO <sub>2</sub>	0.010	0.015	0.022	0.022	0.010	0.015	0.012	0.016	0.059	0.074	0.073	0.012	0.030	0.014	0.005
Al <sub>2</sub> O <sub>3</sub>	0.08	0.29	0.46	0.54	0.20	0.47	0.71	0.33	1.00	1.19	1.27	0.73	0.55	0.37	0.08
FeO	9.37	0.14	0.18	0.35	0.19	0.10	0.25	0.18	0.36	1.82	0.49	0.52	0.96	2.88	0.23
Fe <sub>2</sub> O <sub>3</sub>	37.53	0.34	0.45	0.34	2.07	2.24	1.24	0.82	0.61	0.85	1.82	1.88	0.40	1.26	0.01
Fe <sub>2</sub> O <sub>3</sub> *	43.93	0.50	0.65	0.73	2.28	2.35	1.52	1.02	1.01	2.87	2.36	2.46	1.47	4.46	0.27
MnO	0.15	-	-	-	-	0.05	-	-	-	-	-	-	0.07	3.82	0.06
MgO	0.09	0.02	0.03	0.06	0.02	0.01	0.04	0.01	0.04	0.29	0.01	0.05	0.10	0.16	0.08
CaO	0.05	-	-	0.03	-	-	-	-	-	-	-	-	0.03	0.10	0.05
Na <sub>2</sub> O	0.04	0.04	0.02	0.01	0.03	0.02	0.04	0.01	0.04	0.01	0.03	-	0.02	0.04	-
K <sub>2</sub> O	0.03	0.03	0.04	0.01	0.01	0.01	0.03	0.03	0.18	-	0.02	0.02	0.03	0.03	0.03
P <sub>2</sub> O <sub>5</sub>	0.02	-	-	0.01	-	0.02	0.02	0.01	0.01	0.01	0.02	0.02	0.01	0.05	0.01
H <sub>2</sub> O	0.09	0.19	0.76	0.38	0.03	0.45	0.25	0.24	0.24	2.41	0.49	0.37	0.51	1.05	0.09
CO <sub>2</sub>	-	-	-	-	-	-	-	-	-	-	-	-	-	-	-
Res.	1.63	0.16	-	0.30	0.72	0.02	0.29	0.20	0.71	-	0.21	0.25	0.27	-	0.17
Fe <sub>2</sub> O <sub>3</sub> /FeO	4.0	2.4	2.5	1.0	10.9	22.4	5.0	4.6	1.7	0.5	3.7	3.6	0.4	0.4	<
MnO/Fe <sub>2</sub> O <sub>3</sub> *	<	<	<	<	<	0.02	<	<	<	<	<	<	0.05	0.86	0.22
Al <sub>2</sub> O <sub>3</sub> /TiO <sub>2</sub>	8	19	21	25	20	31	59	21	17	16	17	61	18	26	16
Cr (ppm)	12	33	0	31	16	30	11	23	57	60	70	43	59	16	24
Co	9	2	2	4	5	8	3	1	4	7	1	4	7	13	1
Ni	105	0	4	12	17	19	13	2	21	70	15	25	35	35	0
Cu	102	0	0	1	16	2	0	0	10	5	1	5	33	30	15
Zn	126	3	4	10	7	13	8	6	26	56	11	25	16	39	5
Y	16	4	5	4	5	5	5	9	9	9	7	7	7	8	9
Zr	1	5	7	7	7	7	6	5	14	14	14	4	7	6	2
Nb	9	4	4	4	4	4	4	3	4	5	5	6	5	4	5
Pb	4	0	14	20	51	39	33	4	44	11	8	7	1	3	2

sample	1-Gs	2-B1	2-B2	2-B3	2-B4	2-B5	2-B6	2-B7	2-B8	2-B9	2-B10	2-B11	2-B12	2-Gr1	2-Gr2
SiO <sub>2</sub> (wt%)	62.80	96.77	97.00	89.57	94.62	95.20	92.03	92.93	95.43	91.18	94.72	83.33	84.84	93.68	90.91
TiO <sub>2</sub>	1.220	0.004	0.006	0.004	0.004	0.003	0.004	0.004	0.004	0.005	0.007	0.006	0.004	0.034	0.033
Al <sub>2</sub> O <sub>3</sub>	8.81	0.08	0.07	0.06	0.04	0.05	0.06	0.06	0.01	0.05	0.09	0.08	0.04	0.63	0.67
FeO	9.70	0.27	0.14	0.59	0.27	0.27	0.44	0.52	0.28	0.64	0.57	1.57	2.45	0.57	0.75
Fe <sub>2</sub> O <sub>3</sub>	6.35	0.65	0.28	0.49	0.20	-	0.11	-	-	0.13	1.11	0.32	0.07	1.17	2.88
Fe <sub>2</sub> O <sub>3</sub> *	17.12	0.95	0.44	1.14	0.50	0.30	0.60	0.58	0.31	0.84	1.74	2.06	2.79	1.80	3.71
MnO	0.07	0.02	0.01	0.16	0.03	0.01	0.08	0.09	0.03	0.09	0.01	0.23	0.19	0.02	0.02
MgO	4.80	0.12	0.03	1.57	0.42	0.25	1.01	1.01	0.30	1.36	0.04	1.12	1.79	0.32	0.53
CaO	-	0.27	-	2.94	0.66	0.48	1.76	2.30	0.59	2.33	0.14	7.24	4.81	0.22	0.40
Na <sub>2</sub> O	-	0.01	0.03	-	0.02	0.02	0.01	-	-	0.04	0.06	0.04	0.08	0.01	0.01
K <sub>2</sub> O	0.01	-	-	-	-	-	-	-	-	-	0.02	-	-	0.09	0.04
P <sub>2</sub> O <sub>5</sub>	0.01	0.02	0.01	0.01	0.01	-	0.01	-	0.01	0.01	0.01	0.01	0.02	0.01	0.02
H <sub>2</sub> O	5.17	0.20	1.15	0.27	0.08	0.24	0.12	0.12	0.36	0.07	0.10	0.12	1.00	0.43	0.14
CO <sub>2</sub>	-	0.16	-	3.57	0.42	0.35	1.08	1.85	0.37	1.60	0.22	4.81	3.93	-	0.21
Res.	-	0.64	-	0.09	0.86	0.35	1.52	1.24	0.38	1.43	0.37	1.16	0.50	0.38	1.27
Fe <sub>2</sub> O <sub>3</sub> /FeO	0.7	2.4	2.0	0.8	0.7	<	0.3	<	<	0.2	1.9	0.2	<	2.1	3.8
MnO/Fe <sub>2</sub> O <sub>3</sub> *	<	0.02	0.02	0.14	0.06	0.03	0.13	0.16	0.10	0.11	0.01	0.11	0.07	0.01	0.01
Al <sub>2</sub> O <sub>3</sub> /TiO <sub>2</sub>	7	20	12	15	10	17	15	15	3	10	13	13	10	19	20
Cr (ppm)	23	17	30	33	40	74	35	20	50	25	54	27	38	222	258
Co	32	1	1	2	1	1	1	0	1	0	2	1	4	17	40
Ni	237	0	0	0	0	0	0	0	0	0	5	10	10	125	266
Cu	104	0	0	0	0	0	0	0	0	0	0	1	0	18	26
Zn	141	3	24	30	25	24	27	61	61	65	62	76	38	59	88
Y	33	4	3	5	4	4	6	6	5	7	7	9	7	5	6
Zr	83	3	3	1	1	1	3	0	0	0	2	2	2	4	5
Nb	4	3	4	4	3	2	3	3	3	4	7	5	4	4	4
Pb	19	8	26	31	34	31	32	56	49	54	56	66	40	46	58

sample	2-Gr3	2-Gs1	2-Gs2	3-B1	3-B2	3-B3	3-B4	3-B5	3-B6	3-B7	3-L1	3-L2	3-G	3-PY1	3-PY2
SiO <sub>2</sub> (wt%)	89.68	43.88	50.13	83.17	86.74	31.49	70.09	93.87	96.20	96.88	96.72	95.62	92.70	92.94	93.11
TiO <sub>2</sub>	0.037	0.578	1.490	0.005	0.004	0.008	0.004	0.003	0.006	0.005	0.005	0.015	0.143	0.029	0.027
Al <sub>2</sub> O <sub>3</sub>	0.61	14.38	12.93	0.10	0.07	0.25	0.15	0.05	0.09	0.16	0.16	0.49	3.13	2.17	1.91
FeO	0.95	6.20	13.92	0.23	0.21	2.28	0.83	0.08	0.08	0.03	0.09	0.15	0.19	0.13	0.34
Fe <sub>2</sub> O <sub>3</sub>	3.84	0.32	-	13.02	10.73	62.86	26.69	2.99	0.16	0.21	0.02	0.31	0.46	0.11	0.26
Fe <sub>2</sub> O <sub>3</sub> *	4.89	7.20	15.45	13.28	10.96	65.39	27.61	3.08	0.25	0.24	0.12	0.48	0.67	0.25	0.64
MnO	0.02	0.18	0.23	0.04	0.03	0.04	0.03	0.01	0.01	-	-	0.01	0.02	0.01	0.01
MgO	0.46	4.17	5.35	0.04	0.04	0.04	0.04	0.01	0.01	0.02	-	0.13	0.29	0.14	0.49
CaO	0.46	13.20	5.94	-	-	0.01	-	-	-	-	-	0.01	0.08	-	-
Na <sub>2</sub> O	0.01	0.04	-	0.05	0.03	-	-	0.03	0.03	-	0.02	0.01	-	-	-
K <sub>2</sub> O	0.03	3.96	2.07	-	-	0.01	-	-	-	-	0.02	0.04	0.87	0.62	0.43
P <sub>2</sub> O <sub>5</sub>	0.03	0.06	0.16	0.01	0.02	0.25	0.13	0.01	0.04	0.02	0.01	0.02	0.06	0.01	0.01
H <sub>2</sub> O	0.34	1.94	4.10	1.37	0.84	3.09	2.24	0.23	0.12	0.13	0.06	0.08	0.43	0.13	0.06
CO <sub>2</sub>	-	9.20	2.42	-	-	-	-	-	-	-	-	-	-	-	-
Res.	1.56	0.50	0.41	0.52	0.54	1.27	0.77	0.69	0.48	0.09	0.80	0.30	-	1.01	1.02
Fe <sub>2</sub> O <sub>3</sub> /FeO	4.0	0.1	<	56.6	51.1	27.6	32.2	37.4	2.0	7.0	0.2	2.1	2.4	0.8	0.8
MnO/Fe <sub>2</sub> O <sub>3</sub> *	<	0.03	0.01	<	<	<	<	<	0.04	<	<	0.02	0.03	0.04	0.02
Al <sub>2</sub> O <sub>3</sub> /TiO <sub>2</sub>	16	25	9	20	18	31	38	17	15	32	32	33	22	75	71
Cr (ppm)	147	600	153	21	11	37	28	26	35	37	38	57	576	218	223
Co	48	30	52	3	3	19	5	2	1	1	1	3	2	1	2
Ni	271	158	170	21	14	293	154	4	0	0	0	4	11	5	34
Cu	40	48	119	14	11	68	37	6	0	0	0	2	6	6	7
Zn	114	149	204	78	61	463	238	27	8	4	5	6	20	17	18
Y	8	43	39	11	9	25	7	6	5	5	6	7	18	7	9
Zr	6	54	108	2	2	1	0	2	10	3	23	10	1	4	4
Nb	2	5	4	0	4	2	1	3	4	2	3	4	3	5	3
Pb	68	48	106	8	3	31	6	1	0	20	3	1	34	6	0
sample	4-I1	4-I2	4-I3	4-Sh1	4-Sh2	4-Sh3	4-Ss1	5-I1	5-I2	5-I3	5-I4	5-I5	5-I6	5-I7	5-I8
SiO <sub>2</sub> (wt%)	74.80	88.32	67.53	68.75	78.55	75.03	96.29	42.95	46.80	48.42	50.84	45.39	74.15	80.29	82.83
TiO <sub>2</sub>	0.008	0.005	0.005	1.03	0.38	0.605	0.05	0.097	0.106	0.034	0.020	0.029	0.022	0.018	0.010
Al <sub>2</sub> O <sub>3</sub>	0.14	0.11	0.11	16.88	8.94	13.91	1.10	2.03	2.80	0.85	2.03	1.25	1.62	1.63	1.39
FeO	0.36	0.12	0.27	1.39	1.09	1.63	0.11	1.93	1.86	0.78	0.64	1.53	0.63	0.41	0.45
Fe <sub>2</sub> O <sub>3</sub>	22.75	8.49	30.59	3.57	1.87	1.62	1.63	49.47	44.73	47.59	43.51	49.70	21.10	15.02	12.32
Fe <sub>2</sub> O <sub>3</sub> *	23.15	8.62	30.89	5.11	3.08	3.43	1.75	51.61	46.79	48.46	44.22	51.40	21.80	15.48	12.82
MnO	0.01	0.01	0.01	0.01	0.01	-	-	0.01	0.01	0.04	0.01	0.02	0.03	0.02	0.01
MgO	0.01	0.01	0.09	1.85	2.60	0.61	0.04	0.27	0.62	0.35	0.23	0.18	0.22	0.34	0.09
CaO	0.01	-	0.01	-	0.01	-	-	0.03	0.01	0.03	0.06	0.04	0.01	0.03	-
Na <sub>2</sub> O	-	-	-	0.12	0.06	0.11	0.01	0.19	0.16	0.12	0.25	0.15	0.15	0.14	0.14
K <sub>2</sub> O	-	-	-	4.05	1.88	3.60	0.09	0.47	0.59	0.17	0.19	0.15	0.28	0.25	0.08
P <sub>2</sub> O <sub>5</sub>	0.07	0.02	0.04	0.05	0.02	0.04	0.02	0.04	0.05	0.03	0.05	0.03	0.03	0.02	0.03
H <sub>2</sub> O	0.27	0.12	0.04	1.75	1.06	0.66	0.16	3.37	3.35	2.60	3.15	2.98	1.72	1.21	1.47
CO <sub>2</sub>	-	-	-	-	-	-	-	0.23	0.12	-	-	0.31	0.24	0.11	-
Res.	0.55	0.33	0.44	1.38	1.60	1.55	0.65	-	0.40	0.56	0.22	-	1.27	0.43	0.20
Fe <sub>2</sub> O <sub>3</sub> /FeO	63.2	70.8	113.3	2.6	1.7	1.0	14.8	25.6	24.0	61.0	68.0	32.5	33.5	36.6	27.4
MnO/Fe <sub>2</sub> O <sub>3</sub> *	<	<	<	<	<	<	<	<	<	<	<	<	<	<	<
Al <sub>2</sub> O <sub>3</sub> /TiO <sub>2</sub>	18	22	22	16	24	23	22	21	26	25	102	43	74	91	139
Cr (ppm)	50	39	38	630	389	492	39	39	40	43	108	93	9	2	0
Co	3	1	4	4	7	3	2	4	6	3	4	4	1	1	2
Ni	9	1	10	147	172	24	11	31	30	19	27	22	8	6	12
Cu	26	8	39	27	14	33	18	79	94	68	107	80	50	33	44
Zn	3	3	5	103	173	22	8	109	116	102	86	62	56	38	51
Y	11	6	12	55	22	36	8	31	30	12	21	13	13	11	13
Zr	1	0	1	298	78	112	27	45	51	17	17	16	11	14	10
Nb	3	5	4	13	4	6	3	5	2	9	4	6	4	5	6
Pb	10	0	11	8	6	20	3	33	43	20	65	31	0	6	25

sample	5-19	5-110	5-111	5-112	5-113	5-114	5-Sh1	5-Sh2	5-Sh3
SiO <sub>2</sub> (wt%)	77.98	80.98	87.31	91.94	90.66	90.10	70.16	69.49	67.34
TiO <sub>2</sub>	0.020	0.018	0.006	0.005	0.011	0.013	1.276	1.283	0.787
Al <sub>2</sub> O <sub>3</sub>	1.45	0.49	0.30	0.83	1.11	1.01	13.15	14.77	13.45
FeO	0.48	0.47	0.38	0.31	0.29	0.65	0.39	1.01	1.00
Fe <sub>2</sub> O <sub>3</sub>	17.44	15.67	10.19	6.77	5.24	7.41	6.42	5.52	9.84
Fe <sub>2</sub> O <sub>3</sub> *	17.97	16.19	10.61	7.11	5.56	8.13	6.85	6.64	10.95
MnO	0.01	-	-	0.01	0.01	0.01	-	-	-
MgO	0.10	0.15	0.04	0.07	0.06	0.16	1.26	1.37	1.25
CaO	-	0.44	-	-	-	-	-	-	-
Na <sub>2</sub> O	0.14	0.69	0.15	0.10	0.10	0.22	0.43	0.54	0.52
K <sub>2</sub> O	0.11	0.03	0.03	0.02	0.11	0.07	2.97	2.83	2.82
P <sub>2</sub> O <sub>5</sub>	0.01	0.03	0.01	0.01	0.02	0.01	0.03	0.03	0.02
H <sub>2</sub> O	1.56	1.57	0.82	0.59	0.94	0.86	2.45	3.46	2.60
CO <sub>2</sub>	0.26	0.20	0.14	-	-	-	-	-	-
Res.	0.20	0.18	0.04	0.39	0.28	0.42	1.58	1.02	1.61
Fe <sub>2</sub> O <sub>3</sub> /FeO	36.3	33.3	26.8	21.8	18.1	11.4	16.5	5.5	9.8
MnO/Fe <sub>2</sub> O <sub>3</sub> *	<	<	<	<	<	<	<	<	<
Al <sub>2</sub> O <sub>3</sub> /TiO <sub>2</sub>	73	27	50	166	101	78	10	12	17
Cr (ppm)	3	0	0	11	12	10	105	120	133
Co	1	1	1	0	1	1	2	4	1
Ni	12	4	2	5	3	1	12	13	14
Cu	24	25	19	20	3	11	35	42	70
Zn	50	24	33	24	23	14	34	38	32
Y	15	9	7	9	10	7	44	41	47
Zr	6	11	3	7	4	4	209	198	193
Nb	3	5	5	5	5	4	15	15	13
Pb	9	33	16	11	3	2	37	47	29

Note: The data of CO<sub>2</sub> are listed only for samples containing more than 0.1% CO<sub>2</sub>. - = under the detection limits (0.005%); < = <0.005 for MnO/Fe<sub>2</sub>O<sub>3</sub>\* and <0.05 for Fe<sub>2</sub>O<sub>3</sub>/FeO, respectively; B = banded cherts; G = grey cherts; L = laminated cherts; I = iron formations; Gr = greenish-grey cherts; PY = pale yellowish-grey cherts; Ss = sandstone; Sh = shales; Gs = greenstones. The number, for example 1 of 1-G9, indicates location number (Loc. 1, Marble Bar). See Fig. 1 and Table 1.

TABLE 3

REE data for red cherts from Marble Bar and Pillow Hill

---

sample name	1-B18	2-B10
La (ppm)	0.479	0.151
Ce	0.997	0.417
Pr	0.114	0.054
Nd	0.591	0.279
Sm	0.172	0.083
Eu	0.078	0.040
Gd	0.181	0.093
Tb	0.029	0.019
Dy	0.216	0.139
Ho	0.055	0.032
Er	0.173	0.100
Tm	0.027	0.016
Yb	0.205	0.111
Lu	0.035	0.018

---

TABLE 4

EPMA analyses of rhombic carbonates in a banded chert from Pillow Hill

point	1	2	3	4	5	6	7	8	9	10
MgO(wt%)	12.83	12.22	15.94	16.16	14.75	12.56	13.28	13.27	13.30	17.4
CaO	28.78	29.55	29.95	29.74	29.38	29.30	29.09	28.97	29.03	30.9
FeO	11.43	11.48	5.05	5.28	7.26	10.99	10.79	10.21	10.51	3.59
MnO	0.77	0.85	1.29	1.30	1.35	1.07	0.75	0.65	0.49	1.46
Atomic proportions recalculated as 1(Mg,Ca,Fe,Mn)										
Mg	0.31	0.30	0.40	0.40	0.37	0.31	0.33	0.33	0.33	0.43
Ca	0.51	0.53	0.53	0.53	0.52	0.52	0.52	0.52	0.52	0.55
Fe	0.16	0.16	0.07	0.07	0.10	0.15	0.15	0.14	0.15	0.05
Mn	0.01	0.01	0.02	0.02	0.02	0.02	0.01	0.01	0.01	0.02

TABLE 5

EPMA analyses of hematite in a red chert from Marble Bar

point	1	2	3	4	5	6	7	8	9	10
SiO <sub>2</sub> (wt%)	1.76	2.48	1.63	1.70	1.78	1.83	1.84	1.78	1.94	1.68
TiO <sub>2</sub>	—	0.05	0.01	—	—	—	—	0.04	0.02	0.01
Al <sub>2</sub> O <sub>3</sub>	1.33	1.29	1.31	1.33	1.41	1.34	1.30	1.32	1.30	1.38
FeO	84.60	85.11	86.21	86.94	89.03	87.83	88.94	87.21	87.44	86.82

Note: — = under the detection limit (0.01%).

TABLE 6

Co/Zn and Ni/Zn values in metalliferous deposits

Locations	Co/Zn	Ni/Zn
Marble Bar	0.12(0.06-0.18)	0.76(0.22-1.11)
Roebourne	0.04(0.02-0.05)	0.45(0.23-0.65)
Coppin Gap	0.71(0.33-1.00)	1.78(0.33-3.00)
Point Samson	0.04(0.02-0.06)	0.22(0.06-0.35)
Deep-sea ferromanganese nodules various regions(a)	3.8(1.4-7.4)	7.3(2.6-21.1)
Hydrothermal deposits		
Explorer Ridge(b)	0.07(0.00-0.28)	0.29(0.05-0.58)
Galapagos Rift(c)	0.02(0.01-0.03)	0.35(0.11-0.49)
Santorini, Greece(d)		0.12(0.06-0.26)

Note: (a) Baturin (1988); (b) Grill et al. (1981); (c) Corliss et al. (1978); (d) Boström and Widenfalk (1984).

# 参考論文

- 1 海洋堆積物および陸上堆積岩中の熱水性マンガンマイクロノジュールに関する地球化学的研究。  
杉谷健一郎  
地質学雑誌, 93, 555-574 (1987)
- 2 Compositional variations in manganese micronodules: A possible indicator of sedimentary environments.  
R. Sugisaki, M. Ohashi, K. Sugitani, and K. Suzuki  
Journal of Geology, 95, 433-454 (1987)
- 3 中部日本・美濃帯より産するマンガンバンドの地球化学—海洋堆積物との比較とその地質学的意義—。  
杉谷健一郎  
地質学雑誌, 95, 255-275 (1989)
- 4 New Cu-bearing glass standards for electron microprobe analysis.  
K. Suzuki, I. Kajizuka, K. Yamamoto, M. Ohashi, K. Sugitani and S. Yogo.  
Bull. Nagoya Univ. Furukawa Museum, 6, 21-28 (1990)
- 5 Manganese carbonate bands as an indicator of hemipelagic sedimentary environments.  
R. Sugisaki, K. Sugitani, and M. Adachi  
Journal of Geology, 99, 23-40 (1991)
- 6 Permian hydrothermal deposits in the Mino Terrane, central Japan: implications for hydrothermal plumes in an ancient ocean basin.  
K. Sugitani, H. Sano, M. Adachi and R. Sugisaki  
Sedimentary Geology, 71, 59-71 (1991)